

## Electronic, optical, and structural properties of some wurtzite crystals

Yong-Nian Xu and W. Y. Ching

*Department of Physics, University of Missouri—Kansas City, Kansas City, Missouri 64110*

(Received 21 January 1993)

Using the first-principles orthogonalized linear-combination-of-atomic orbitals method in the local-density approximation, the electronic structures and the linear-optical properties of ten wurtzite crystals, BeO, BN, SiC, AlN, GaN, InN, ZnO, ZnS, CdS, and CdSe are investigated. Results on band structures, density of states, effective masses, charge-density distributions, and effective charges are presented and compared. Optical properties of the ten wurtzite crystals up to a photon energy of 40 eV are calculated and the dielectric functions are resolved into components perpendicular and parallel to the  $z$  axis. The calculated results are compared with the available experimental data and other recent calculations. The structural properties of the wurtzite crystals are also studied by means of local-density total-energy calculations. It is shown that the calculated equilibrium volume and the bulk modulus are in good agreement with recent experimental data.

### I. INTRODUCTION

In comparison with III-V semiconductors with a zincblende (ZB) structure, binary semiconductors and insulators with a wurtzite ( $W$ ) structure have not been widely studied.<sup>1</sup> In the ideal case in which the  $c/a$  ratio equals 1.6333 and the internal parameter  $u=0.375$ , the  $W$  structure differs from the ZB structure only in the stacking sequence of the  $A$ - $B$  atoms in the [111] direction of the compound  $AB$ . For most  $W$  crystals, the  $c/a$  ratio and  $u$  deviate slightly from the ideal values which result in two slightly different nearest-neighbor distances: one with a length of  $uc$  and the other three of length  $[a^2/3 + (\frac{1}{2}-u)^2c^2]^{1/2}$ . Many semiconductor crystals such as SiC, ZnS, CdS, etc., exist in both forms. The local atomic environments in both crystals are sufficiently close and it has been taken for granted that their electronic structures should also be very similar. Nevertheless, the lower symmetry in the  $W$  structure (space-group  $P6_3mc$ ) does result in new features in electronic properties that are unique only to  $W$  crystals.

In this paper, we report the results of a detailed study of the electronic and optical properties of ten wurtzite crystals using the self-consistent orthogonalized linear-combination-of-atomic-orbitals (OLCAO) method. The  $W$  crystals are BeO, BN, SiC, AlN, GaN, InN, ZnO, ZnS, CdS, and CdSe. With the exception of BN, which crystallizes in hexagonal and cubic phases, all these crystals have the  $W$  structure as the stable phase. At high pressure, hexagonal BN may transform into the  $W$  structure. Our main objective is to have a comprehensive set of results obtained by a state-of-the-art method that could be the basis for further studies in these materials. In 1985, Huang and Ching<sup>2</sup> presented the band structures of six of these  $W$  crystals plus 28 other semiconductors with 17 of them in the ZB structure using the OLCAO method. However, the calculations in that study were not self-consistent and a minimal basis set was used. In the spirit of a semi-*ab-initio* approach, the exchange parameter in the one-electron atomlike  $X$ - $\alpha$  potential was

adjusted so as to reproduce the experimental band gap for each crystal. The semi-*ab-initio* approach with a minimal basis set gave results far more superior than the semiempirical tight-binding method with only a modest increase in computational effort. The transferability of the basis set and the potential makes it ideal for studying more complex configurations of the semiconductor systems and compounds,<sup>3-7</sup> or for more demanding calculations such as nonlinear optical properties.<sup>8,9</sup>

In the last few years, the methodology of the OLCAO method has been greatly refined and improved. Fully self-consistent, first-principles calculations with a full basis set have been carried out by our group in a large number of crystals<sup>10</sup> including semiconductors,<sup>11-13</sup> insulators,<sup>14,24</sup> high- $T_c$  superconductors,<sup>25-30</sup> ferroelectric crystals,<sup>31,34</sup> metals and metallic compounds,<sup>35,36</sup> fullerene and related systems,<sup>37-42</sup> etc., many of them with very complex crystal structures. It is therefore timely to reinvestigate the electronic properties of wurtzite crystals as a distinctive group. It is not uncommon to find detailed calculations in the published literature that are devoted to one or two wurtzite crystals. We find it more substantial and useful to present the results of ten  $W$  crystals in a single publication so that a meaningful comparison can be made easier. Our present results include band structures, density of states (DOS), effective masses, charge distributions and bonding patterns, total-energy calculations, and linear-optical properties. The result for AlN is repetitious and is a continuation of the study by Ching and Harmon in 1986.<sup>14</sup> The optical result for AlN has also been presented in conjunction with experimental measurement and critical-point modeling.<sup>43</sup> The result for BN has been reported earlier in which the three phases of BN,<sup>20</sup> ZB,  $W$ , and hexagonal, were studied.

Almost all of the ten  $W$  crystals are materials of increasing importance in modern technology. BeO is a pyroelectric material composed of very light elements. BN and SiC are known for their superior mechanical properties that are especially valuable in high-temperature applications.<sup>44,45</sup> Although the stable phase for BN is the

hexagonal phase and SiC has a number of polytypes with ZB being the most common one, the  $W$  phase is important in connection with stability in the epitaxial growth of thin films and in the structural phase transitions under pressure. The III-V nitrides AlN, GaN, and InN and their alloys have promising applications in semiconductor technology because of their larger band gaps in comparison with cubic III-V compound semiconductors.<sup>46</sup> AlN is also a very important ceramic material noted for its excellent mechanical, thermal, temperature-resistant, and piezoelectric properties.<sup>47,48</sup> GaN has gained much attention recently because of its potential as a blue light emitter due to a wider band gap.<sup>46</sup> InN has been given very little attention because of material problems associated with defect contamination and other technical difficulties in the growth process.<sup>46</sup> The application of II-VI compounds (ZnO, ZnS, CdS, CdSe) and their alloys in either ZB or  $W$  structures are mainly in electro-optical and electro-acoustic devices.<sup>49–52</sup> When doped with Mn, the Zn-based  $W$  crystals form an interesting group of dilute magnetic semiconductors.

The layout of the paper is as follows. In the next section, we give a brief sketch of the method of calculation. The electronic structure results for ten  $W$  crystals are presented in Sec. III. In Sec. IV, we make a detailed analysis of the charge distribution and the effective charges in these crystals. The results of optical properties are presented and discussed in Sec. V and that of the total-energy calculation in Sec. VI. Some conclusions are drawn in the last section.

## II. METHOD OF CALCULATION

The first-principles self-consistent OLCAO method in the local-density approximation for electronic structure determination, total-energy calculation, and optical property studies of crystals has been described in the published literature.<sup>10</sup> We shall only briefly mention those points that are relevant to the present calculation for  $W$  crystals. The Kohn-Sham form of the exchange-correlation potential<sup>53</sup> with Wigner interpolation formula for additional exchange effects is used.<sup>54</sup> We employ a full basis set consisting of linear combinations of atomic

orbitals expressed as a sum of Gaussian-type orbitals. In the present calculation, the  $3d$  orbitals of Zn, Ga, and Se, and the  $4d$  orbitals of Cd and In are treated as valence orbitals. Extra orbitals corresponding to excited states for each atom are included to ensure sufficient convergence in the basis set expansion. The atomic basis orbitals used for the ten wurtzite crystals are listed in Table I.

In the direct-space OLCAO method, the potential and charge-density functions are also expressed in a form of a sum of atom-centered Gaussian functionals<sup>10</sup> with fixed exponentials. We have adopted a set of 16 Gaussians per site with exponentials ranging from 0.1 to 100 000. The accuracy of the calculation depends very sensitively on the accuracy of the charge-density fit. In the present calculations for  $W$  crystals, we have achieved a fitting accuracy of no worse than 0.004 electrons per valence electron. This level of accuracy is very adequate for the band-structure and optical properties calculations. Fortunately, this fitting error is more or less stable for each crystal at different volume contractions so the relative error introduced in the total energy is much smaller. In the self-consistent iteration, a total of 12 special  $k$  points are  $\frac{1}{24}$  in the Brillouin zone (BZ) were used. For the density of states (DOS) and optical calculations, energy eigenvalues and wave functions were obtained at 95 regularly spaced  $k$  points in the same irreducible portion of the BZ. For the DOS calculation, the linear analytic tetrahedron method<sup>55</sup> was used. Spin-orbit interaction was not included in the present calculation and this may affect the calculated effective masses and gaps for  $W$  crystals containing heavy elements.

For the optical calculation, the real part of the frequency-dependent interband optical conductivity  $\sigma(\omega)$  was evaluated first with all the optical transition matrix elements between the unoccupied valence bands (VB's) and the occupied conduction bands (CB's) fully included. From the  $\sigma(\omega)$  curve, the real and the imaginary parts of the dielectric function,  $\epsilon_1(\omega)$ ,  $\epsilon_2(\omega)$ , and the electron energy-loss (ELF) function were extracted.<sup>10</sup>

For the total-energy calculation, we assume a condition of isotropic strain. Hence, the symmetry, the  $c/a$  ratios, and the internal parameters of the  $W$  crystals were kept the same, and only the lattice constants were scaled. The

TABLE I. Atomic orbitals used in the OLCAO basis set for elements in the wurtzite calculation.

Element	Z	Core orbitals	Valence orbitals	Additional orbitals
Be	4	1s	2s, 2p	3s, 3p
B	5	1s	2s, 2p	3s, 3p
C	6	1s	2s, 2p	3s, 3p
N	7	1s	2s, 2p	3s, 3p
O	8	1s	2s, 2p	3s, 3p
Al	13	1s, 2s, 2p	3s, 3p	4s, 4p, 3d
Si	14	1s, 2s, 2p	3s, 3p	4s, 4p, 3d
S	16	1s, 2s, 2p	3s, 3p	4s, 4p, 3d
Zn	30	1s, 2s, 2p, 3s, 3p	4s, 4p, 3d	5s, 5p, 4d
Ga	31	1s, 2s, 2p, 3s, 3p	4s, 4p, 3d	5s, 5p, 4d
Se	34	1s, 2s, 2p, 3s, 3p	4s, 4p, 3d	5s, 5p, 4d
Cd	48	1s, 2s, 2p, 3s, 3p, 4s, 4p, 3d	5s, 5p, 4d	6s, 6p, 5d
In	49	1s, 2s, 2p, 3s, 3p, 4s, 4p, 3d	5s, 5p, 4d	6s, 6p, 5d

total energy  $E$  of the crystal was evaluated as a function of the volume fractions  $V/V_0$ , where  $V_0$  is the experimental equilibrium volume. Based on the calculated  $E$  versus  $V/V_0$  data points, the bulk static properties of the  $W$  crystals were obtained by fitting the calculated data to Murnaghan's equation of state.<sup>56</sup> The bulk modulus  $B$ , the pressure coefficient  $B'$ , and the crystal volume  $V_{\min}$  where the calculated total energy is a minimum were obtained.

In a real situation, a uniform hydrostatic pressure leads to isotropic compression which may induce changes in the  $c/a$  ratio and the internal parameter. A more sophisticated and demanding first-principles calculation will involve geometry optimization. The present total-energy calculation corresponds to an idealized situation that closely mimics the real one near equilibrium.

### III. ELECTRONIC STRUCTURES

As mentioned earlier, there were not many rigorous calculations of electronic structures for  $W$  crystals. We summarize briefly some of the recent results of electronic structure studies for  $W$  crystals. Recently, Yeh *et al.* considered the problem of ZB- $W$  polytypism in several semiconductors using the local-density calculation.<sup>57</sup> Chang, Froyen, and Cohen studied the BeO crystal using the first-principles pseudopotential method.<sup>58,59</sup> Continenza, Wentzcovitch, and Freeman explored the possibility of a graphitic form of BeO using the first-principles local-density approximation (LDA) calculation.<sup>60</sup> Posternak and co-workers addressed the problem of spontaneous polarization in BeO using the ground-state first-principles theory.<sup>61</sup> Park, Terakura, and Hamada were the first to calculate electronic structures for all three phases of BN including the  $W$  structure.<sup>62</sup> Lam, Wentzcovitch, and Cohen studied the possibility of phase transition in BN from the hexagonal structure to the  $W$  structure at high pressure.<sup>63</sup> A comparison of band structures of SiC, AlN, and GaN in  $W$  and ZB crystals was attempted by Lambrecht and Segall (LS).<sup>64</sup> Bulk structural properties of AlN have also been studied by Gorczyca *et al.*<sup>65</sup> and Van Camp, Van Doren, and Devreese.<sup>66</sup> Min, Chan, and Ho (MCH) studied the bulk properties of GaN using the total-energy pseudopotential calculation.<sup>67</sup> Earlier calculations gave rather different band structures for GaN.<sup>68-70</sup> Perlin *et al.*<sup>71</sup> presented the pressure-dependent properties for GaN. Muñoz and Kunc<sup>72</sup> studied the high-pressure phase transition in GaN using the local-density pseudopotential calculation. For InN, Foley and Tansley did an empirical pseudopotential calculation in 1986.<sup>73</sup> Jenkins and Dow studied the electronic structures of InN, InGaN, InAlN, and the effect of doping in these systems using a nearest-neighbor tight-binding model.<sup>74</sup> The band structure of ZnO was studied using the empirical pseudopotential<sup>75</sup> and also the nonlocal pseudopotential methods<sup>76</sup> quite a long time ago. Mishra and co-workers investigated the fundamental issue of "bands versus bonds" in ZnO using the  $X\text{-}\alpha$  multiple-scattering method for the cluster calculation and the augmented-spherical-wave calculation for the band structures.<sup>77</sup> The electronic structures of wurtzite ZnS,

CdS, and CdSe were first calculated by the empirical pseudopotential method in the 1960s.<sup>78-80</sup> We are unable to locate more recent calculations for ZnS, CdS, and CdSe in the  $W$  structure other than the semi-*ab-initio* OLCAO calculation mentioned above.<sup>2</sup>

Our calculated band structures for the ten  $W$  crystals are shown in Figs. 1–10. The corresponding DOS which is resolved into atomic components is presented in Figs. 11–20. The lattice constants  $a$ ,  $c$ , and the internal parameter  $u$  used in the present calculation are listed in Table I. These are all experimentally determined values from various sources such as those listed in Ref. 2. All the  $W$  crystals are insulating with finite band gaps and the zero of the energy is thus set at the top of the VB. The VB consists of a  $p$ -orbital dominated upper VB and an  $s$ -orbital dominated lower VB. In the cases of GaN, InN, ZnO, ZnS, CdS, and CdSe, additional narrow bands corresponding to the semicorelike  $3d$  or  $4d$  states are also present in the VB. Of the ten crystals, BN and SiC show indirect band gaps with the top of the VB at the zone center  $\Gamma$  and the bottom of the CB at  $K$ . All other crystals have direct band gaps at  $\Gamma$ . The calculated gap values are listed in Table I together with the known measured values.<sup>52,69,81-84</sup> As expected from the local-density calculations, the calculated band gap underestimates the measured value by a low percentage value of 3% in CdSe to a high value of 73% in ZnO. In cubic semiconductors, gap underestimation over 100% using the LDA calculation is quite common.<sup>13</sup> Also listed in Table I are the total VB width and the widths of the separated bands  $W1$ ,  $W2$ , and  $W3$  within the VB region, as well as the gaps separating them ( $G1$ ,  $G2$ ). From the DOS diagrams, it is obvious that the  $3d$  or  $4d$  electrons

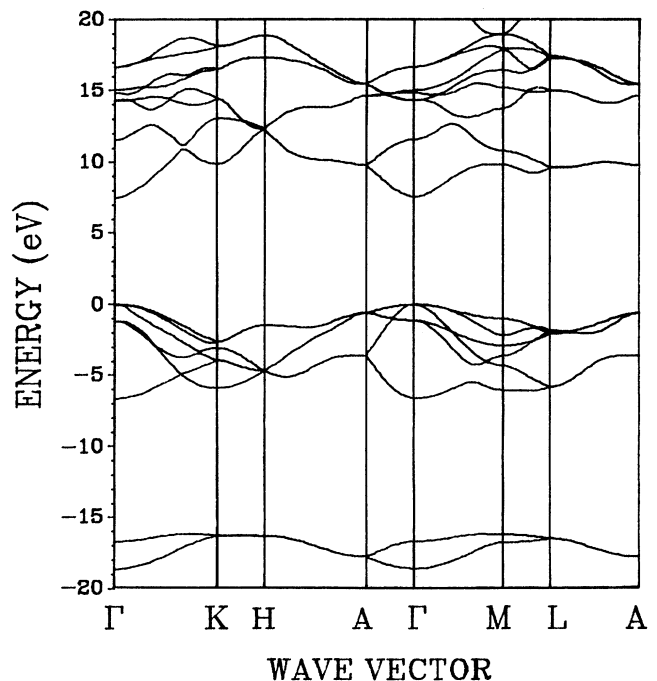


FIG. 1. Calculated band structure of BeO.

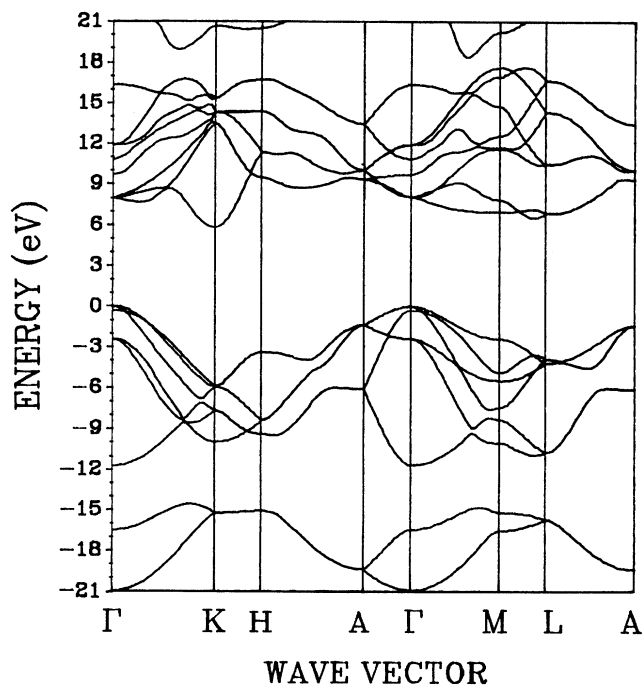


FIG. 2. Calculated band structure of BN.

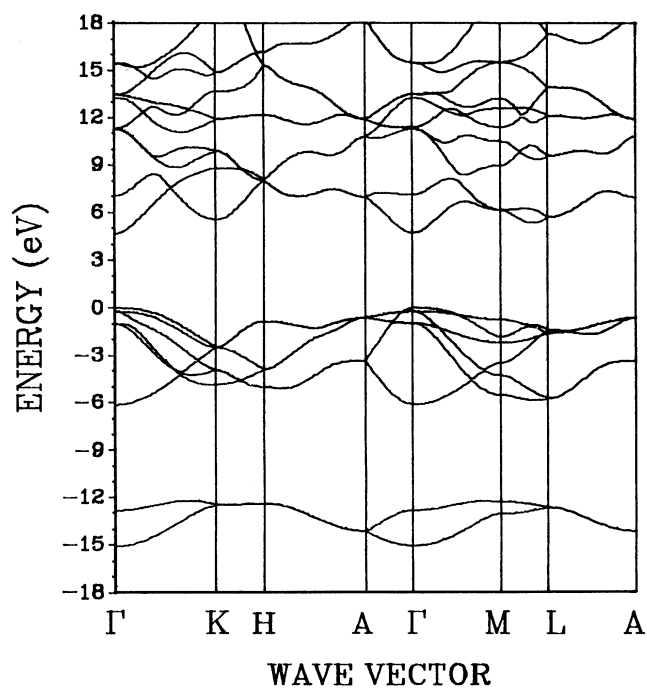


FIG. 4. Calculated band structure of AlN.

from the cations interact with the valence electrons of the anion, and should never be treated as the core electrons were in the case of some older calculations.

For BeO, our OLCAO result is very close to the first-principles pseudopotential calculation of Chang, Froyen, and Cohen.<sup>58</sup> They obtained a direct gap of 7.0 eV and a

total VB width of 19.0 eV versus our value of 7.54 and 18.67 eV, respectively. For GaN, our calculated direct gap of 2.71 eV is close to the recent first-principles pseudopotential calculation of MCH who also obtained a direct band gap of 3.0 eV.<sup>67</sup> LS compared the electronic structures of SiC, AlN, and GaN in the ZB and *W* struc-

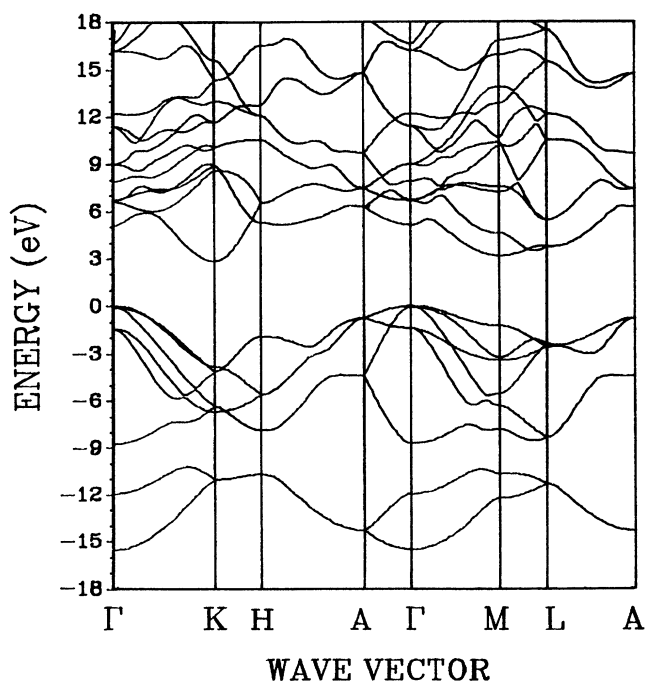


FIG. 3. Calculated band structure of SiC.

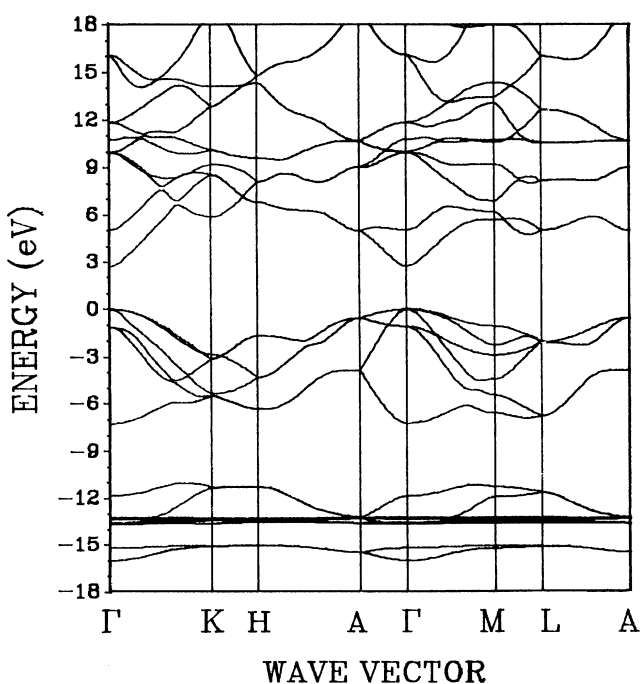


FIG. 5. Calculated band structure of GaN.

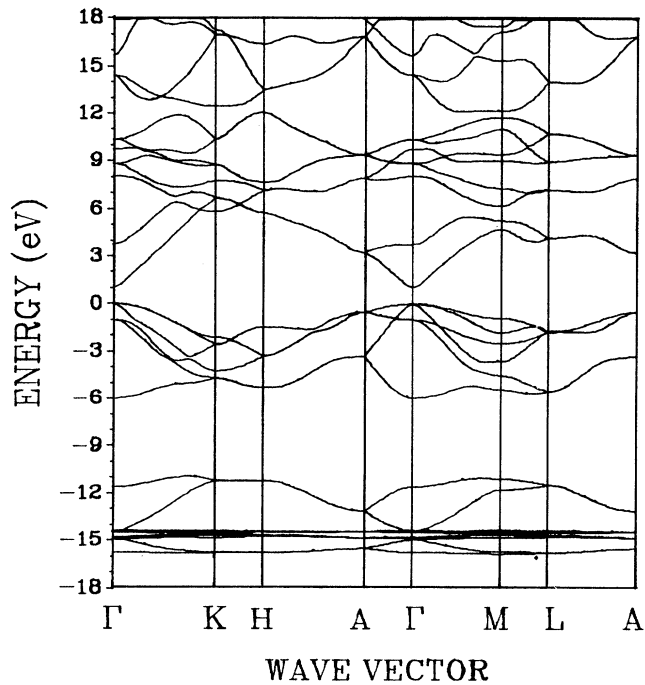


FIG. 6. Calculated band structure of InN.

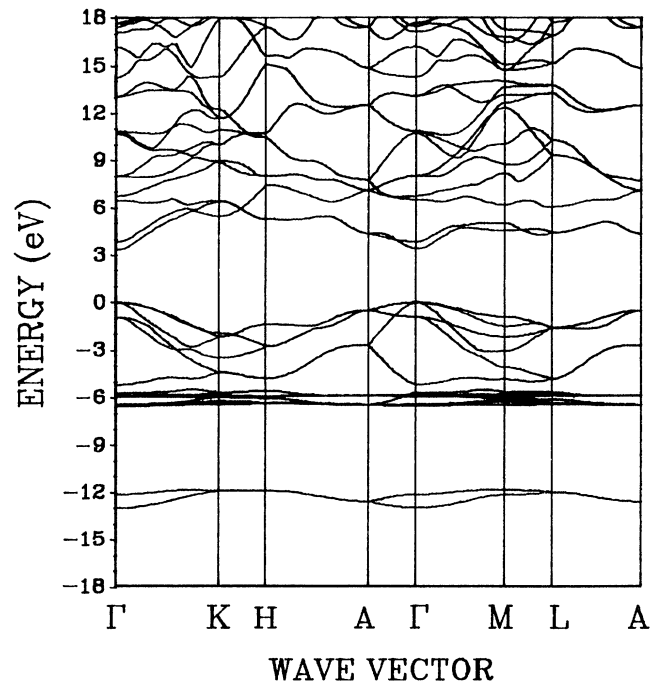


FIG. 8. Calculated band structure of ZnS.

tures using the LMTO method.<sup>64</sup> They obtained gap values for the *W* phase without the *GW* correction to be the following: SiC, indirect gap of 2.67 eV; AlN, direct gap of 4.94 eV; and GaN, direct gap of 2.75 eV. These values are very close to our calculated values listed in Table II. Ley *et al.* measured the VB DOS of a large

number of III-V and II-VI compounds using x-ray photoelectron spectroscopy,<sup>84</sup> of which three were for *W* crystals (ZnO, CdS, and CdSe). Our calculated DOS is in general good agreement with their data, although the experimental curves have rather low resolution and only a general comparison is possible.

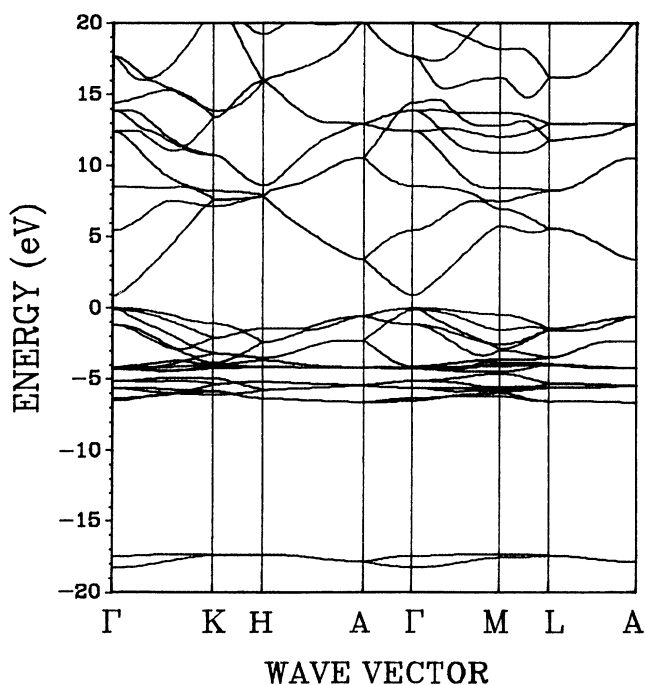


FIG. 7. Calculated band structure of ZnO.

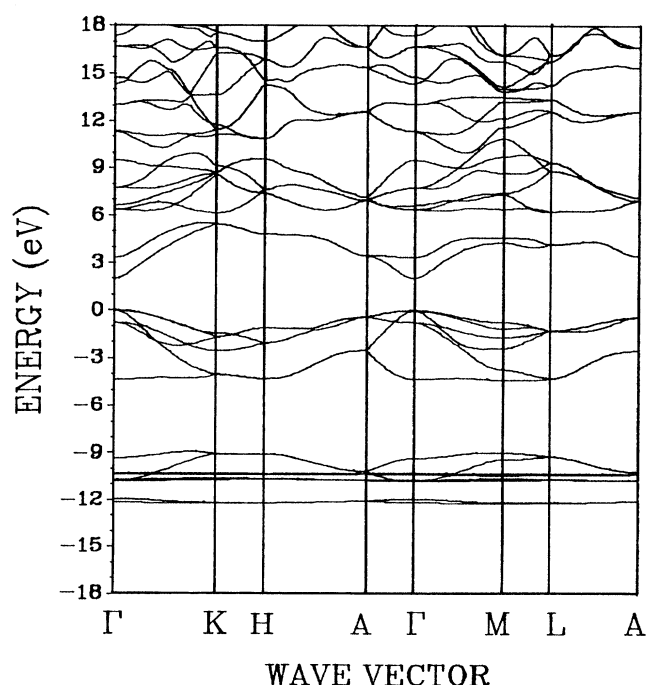


FIG. 9. Calculated band structure of CdS.

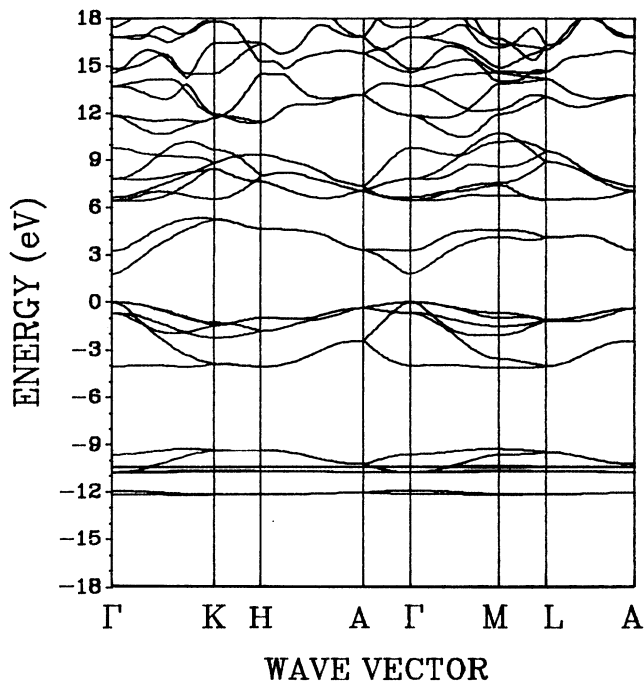


FIG. 10. Calculated band structure of CdSe.

The effective mass for the electrons in the CB and the holes in the VB are also evaluated from the band curvatures for the  $W$  crystals. The effective masses are highly anisotropic. In Table III, we list the effective-mass components along the three symmetry axes,  $\Gamma$ - $M$ ,  $\Gamma$ - $A$  and  $\Gamma$ - $K$ . For BN and SiC, the bottom of CB is at  $K$  so the components for the electron effective mass are evaluated along the  $K$ - $H$  and the  $K$ - $\Gamma$  directions. Several interesting points are obvious: (1) The holes are much heavier

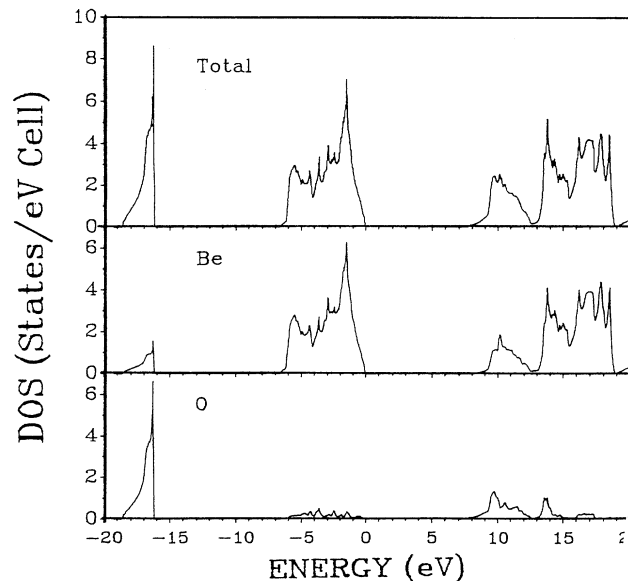


FIG. 11. Calculated DOS and partial density of states (PDOS) of BeO.

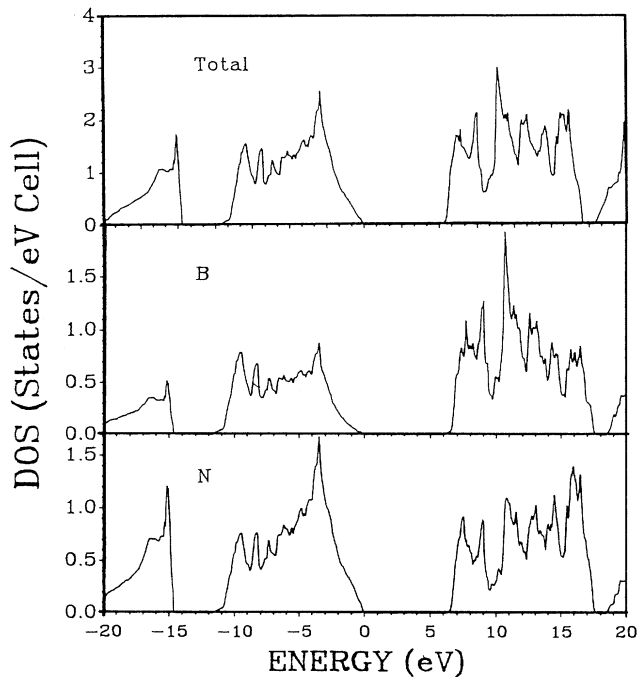


FIG. 12. Calculated DOS and PDOS of BN.

than the electrons. The large disparity in the electron and hole mobilities can result in larger optical nonlinearity in these crystals. (2) The hole effective masses are more anisotropic. This is related to the fact that the top of the VB is associated with the  $p$  orbitals of the anions. (3) The electron effective masses are generally less than 0.5 electrons except in the case of BeO. Carrier transport in these crystals should be dominated by electrons. (4) The electron effective mass has the smallest component along the  $k_z$  direction, a fact that may be of importance in the film and superlattice construction of these crystals. (5) Several crystals (BeO, AlN, ZnO) have very large hole

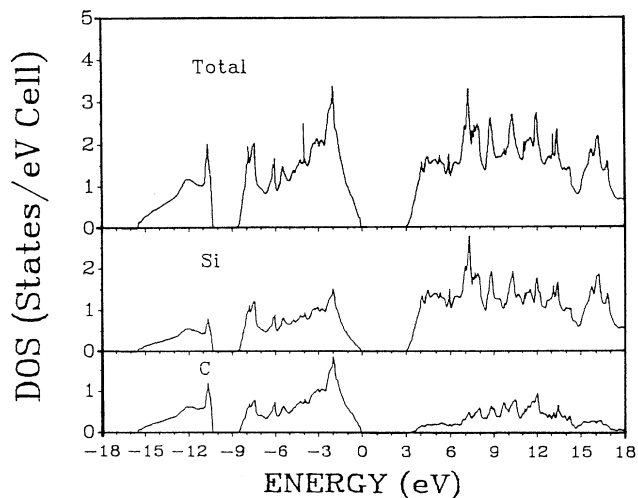


FIG. 13. Calculated DOS and PDOS of SiC.

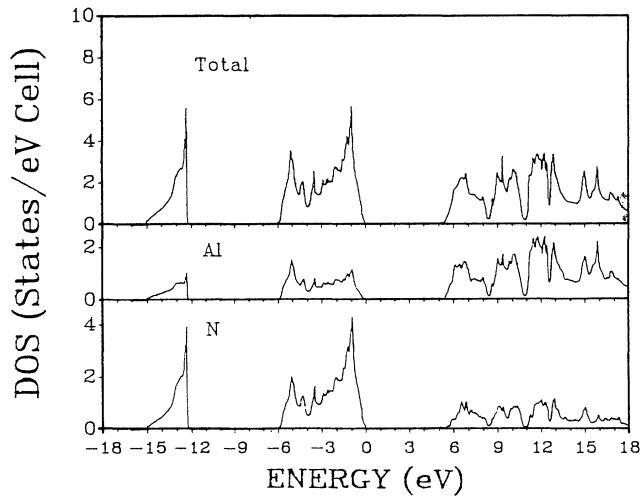


FIG. 14. Calculated DOS and PDOS of AlN.

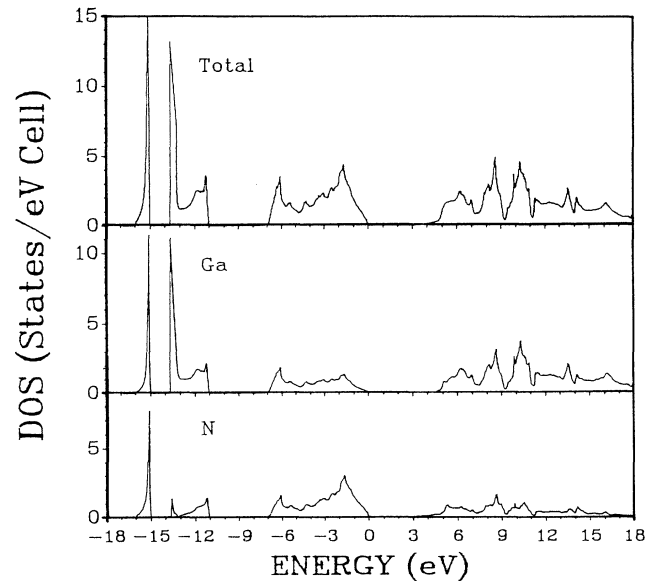


FIG. 15. Calculated DOS and PDOS of GaN.

TABLE II. Experimental lattice parameters, calculated bandwidths, and gaps for some wurtzite crystals.

Crystal	Lattice (Å)	Total	W1	VB width (eV)			G1	G2	Gap (eV)	
				W2	W3	Calculated			Experiment	
BeO	$a=2.698$ $c=4.380$ $u=0.378$	18.67	6.66	2.50		9.45		7.54( <i>d</i> )	10.6 <sup>c</sup> 7–10.7 <sup>h</sup>	
BN	$a=2.536$ $c=4.199$ $u=0.375$	21.00	11.76	6.28		2.93		5.81( <i>id</i> ) 8.00( <i>d, Γ</i> )		
SiC	$a=3.076$ $c=5.048$ $u=0.375$	15.53	8.79	5.33		1.41		2.82( <i>id</i> ) 5.10( <i>d, Γ</i> )	3.33 <sup>a</sup> 2.86 <sup>c</sup>	
AlN	$a=3.110$ $c=4.980$ $u=0.382$	15.11	6.16	2.89		6.07		4.64( <i>d</i> )	6.28 <sup>a</sup>	
GaN	$a=3.190$ $c=5.189$ $u=0.375$	16.03	7.26	2.65	0.98	3.76	1.39	2.71( <i>d</i> )	3.50 <sup>f</sup> 3.60 <sup>b</sup>	
InN	$a=3.533$ $c=5.692$ $u=0.375$	15.78	5.98	4.84		4.95		1.02( <i>d</i> )	1.90 <sup>g</sup>	
ZnO	$a=3.249$ $c=5.207$ $u=0.345$	18.28	6.67	0.98		10.63		0.88( <i>d</i> )	3.30 <sup>c</sup>	
ZnS	$a=3.811$ $c=6.234$ $u=0.375$	13.00	6.54	1.08	1.17	0.26	5.30	3.35( <i>d</i> )	3.91 <sup>e</sup>	
CdS	$a=4.137$ $c=6.7144$ $u=0.375$	12.25	4.43	1.89	0.32	4.55	1.11	2.02( <i>d</i> )	2.58 <sup>d</sup> 2.4 <sup>c</sup>	
CdSe	$a=4.2985$ $c=7.0152$ $u=0.375$	12.24	4.18	1.56	0.31	5.10	1.11	1.79( <i>d</i> )	1.84 <sup>d</sup> 1.80 <sup>c</sup>	

<sup>a</sup>Reference 81.<sup>b</sup>Reference 69.<sup>c</sup>Table 1.1.1.2 in Ref. 52.<sup>d</sup>As cited in Ref. 84.<sup>e</sup>For cubic ZnS, Table 1.1.1.2 in Ref. 52.<sup>f</sup>Reference 82.<sup>g</sup>Reference 83.<sup>h</sup>As listed in Ref. 58.

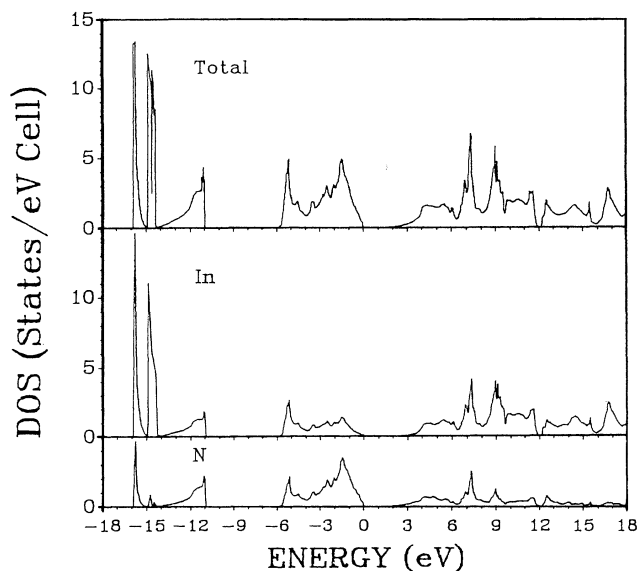


FIG. 16. Calculated DOS and PDOS of InN.

effective masses and conduction by holes in these crystals can be ruled out. (6) In the AlN, GaN, and InN series, the electron effective masses become progressively smaller as the cation becomes heavier. This is in line with the high electron mobility observed in pure InN samples.<sup>85</sup>

#### IV. EFFECTIVE CHARGES

The effective charges  $Q_A^*$  and  $Q_B^*$  on atoms  $A$  and  $B$  in a binary compound  $AB$  is a very useful concept to inter-

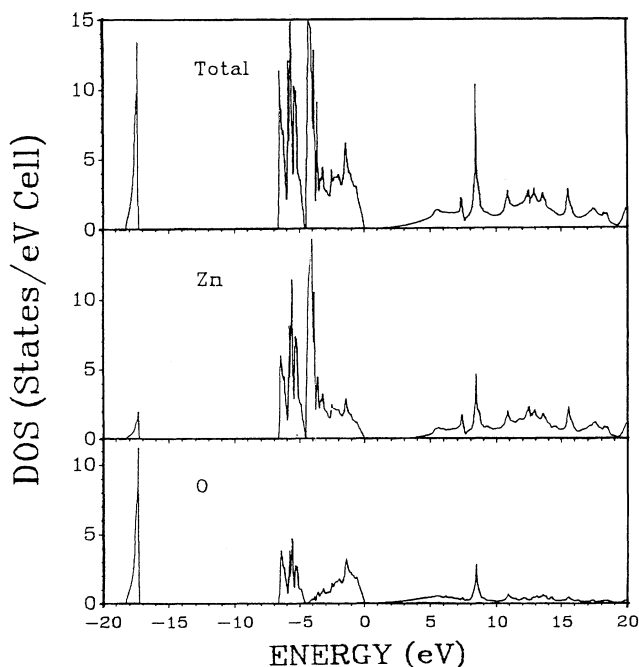


FIG. 17. Calculated DOS and PDOS of ZnO.

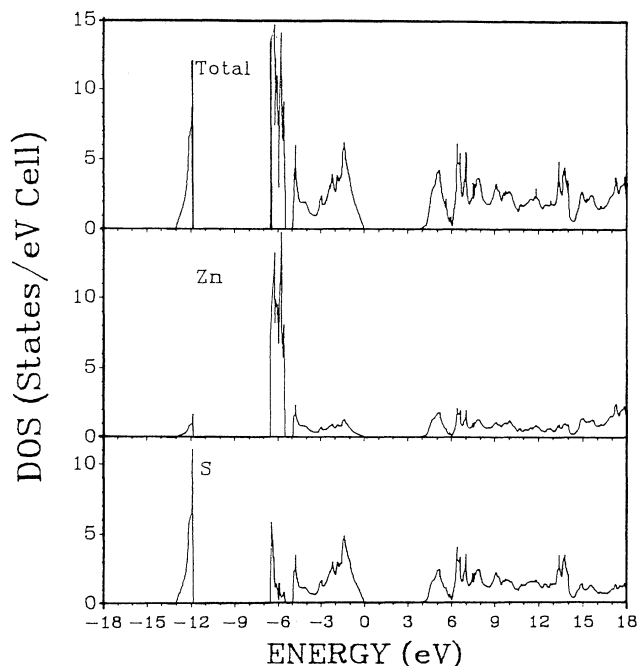


FIG. 18. Calculated DOS and PDOS of ZnS.

pret many physical phenomena in these crystals.<sup>86</sup> For example, the fractional ionic character (FIC) is defined as

$$\text{FIC} = |Q_A^* - Q_B^*| / (Q_A^* + Q_B^*) \quad (1)$$

which ranges from 0 for a perfectly covalent compound to 1 for a 100% ionic compound. The simplest way to obtain  $Q_A^*$  and  $Q_B^*$  in a LCAO-type of calculation is to use the Mulliken population analysis scheme.<sup>87</sup> However, the Mulliken scheme is an approximate one which assumes the equal sharing of the overlap between the atoms in the crystal. When the basis set is reasonably localized

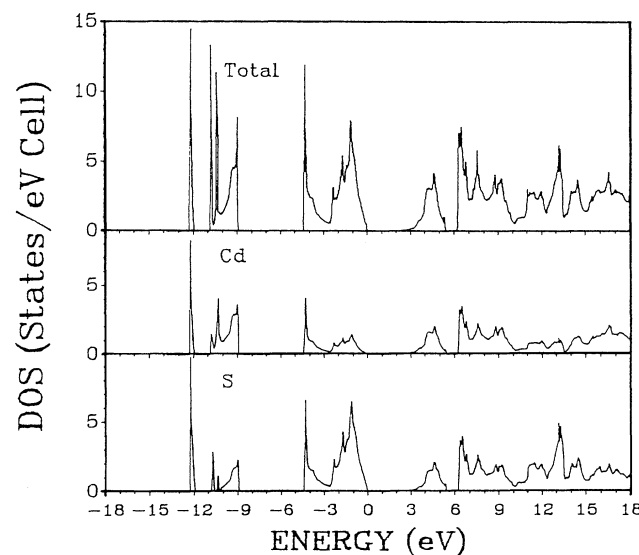


FIG. 19. Calculated DOS and PDOS of CdS.



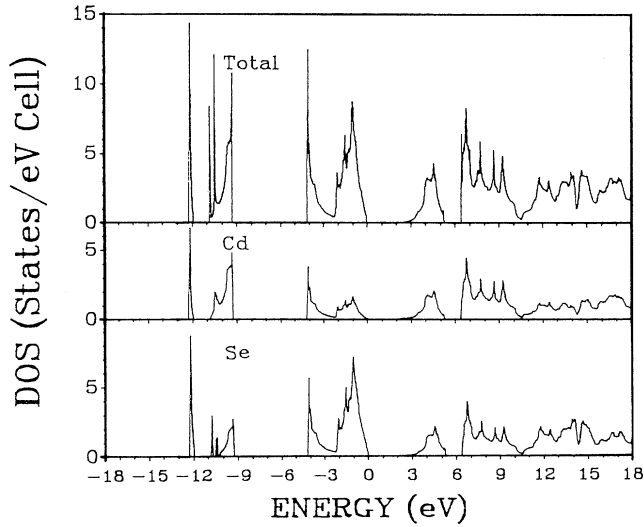


FIG. 20. Calculated DOS and PDOS of CdSe.

such as in a minimal basis calculation,<sup>2</sup> the Mulliken scheme can give quite reliable values for  $Q_A^*$  and  $Q_B^*$ . However, in a more precise calculation, such as this one in which a full basis set is used, the Mulliken scheme can fail miserably because of the large overlap of the extend-

TABLE III. Calculated effective-mass components for wurtzites (in units of electron mass).

Crystal	CB edge	VB edge
BeO	0.75 ( $\Gamma \rightarrow K$ )	-2.44 ( $\Gamma \rightarrow K$ )
	0.58 ( $\Gamma \rightarrow A$ )	-12.01 ( $\Gamma \rightarrow A$ )
BN	0.73 ( $\Gamma \rightarrow M$ )	-2.44 ( $\Gamma \rightarrow M$ )
	0.35 ( $K \rightarrow \Gamma$ )	-0.88 ( $\Gamma \rightarrow K$ )
	0.24 ( $K \rightarrow H$ )	-1.08 ( $\Gamma \rightarrow A$ )
SiC	0.54 ( $K \rightarrow \Gamma$ )	-1.02 ( $\Gamma \rightarrow M$ )
	0.29 ( $K \rightarrow H$ )	-1.31 ( $\Gamma \rightarrow K$ )
AlN	0.42 ( $\Gamma \rightarrow K$ )	-1.54 ( $\Gamma \rightarrow A$ )
	0.33 ( $\Gamma \rightarrow A$ )	-1.83 ( $\Gamma \rightarrow M$ )
	0.40 ( $\Gamma \rightarrow M$ )	-3.40 ( $\Gamma \rightarrow K$ )
GaN	0.36 ( $\Gamma \rightarrow K$ )	-0.30 ( $\Gamma \rightarrow A$ )
	0.27 ( $\Gamma \rightarrow A$ )	-3.52 ( $\Gamma \rightarrow M$ )
	0.33 ( $\Gamma \rightarrow M$ )	-1.58 ( $\Gamma \rightarrow K$ )
InN	0.31 ( $\Gamma \rightarrow K$ )	-2.03 ( $\Gamma \rightarrow A$ )
	0.20 ( $\Gamma \rightarrow A$ )	-1.93 ( $\Gamma \rightarrow M$ )
	0.26 ( $\Gamma \rightarrow M$ )	-1.51 ( $\Gamma \rightarrow K$ )
ZnO	0.37 ( $\Gamma \rightarrow K$ )	-1.84 ( $\Gamma \rightarrow A$ )
	0.28 ( $\Gamma \rightarrow A$ )	-1.73 ( $\Gamma \rightarrow M$ )
	0.32 ( $\Gamma \rightarrow M$ )	-4.31 ( $\Gamma \rightarrow K$ )
ZnS	0.35 ( $\Gamma \rightarrow K$ )	-1.98 ( $\Gamma \rightarrow A$ )
	0.26 ( $\Gamma \rightarrow A$ )	-4.94 ( $\Gamma \rightarrow M$ )
	0.33 ( $\Gamma \rightarrow M$ )	-1.33 ( $\Gamma \rightarrow K$ )
CdS	0.26 ( $\Gamma \rightarrow A$ )	-1.51 ( $\Gamma \rightarrow A$ )
	0.33 ( $\Gamma \rightarrow M$ )	-1.47 ( $\Gamma \rightarrow M$ )
	0.27 ( $\Gamma \rightarrow K$ )	-1.41 ( $\Gamma \rightarrow K$ )
CdSe	0.21 ( $\Gamma \rightarrow A$ )	-1.41 ( $\Gamma \rightarrow K$ )
	0.25 ( $\Gamma \rightarrow M$ )	-1.53 ( $\Gamma \rightarrow A$ )
	0.24 ( $\Gamma \rightarrow K$ )	-1.50 ( $\Gamma \rightarrow M$ )
	0.18 ( $\Gamma \rightarrow A$ )	-1.44 ( $\Gamma \rightarrow K$ )
	0.22 ( $\Gamma \rightarrow M$ )	-1.60 ( $\Gamma \rightarrow A$ )
		-1.52 ( $\Gamma \rightarrow M$ )

ed orbitals of the atoms. In this case, a better way of determining  $Q_A^*$  and  $Q_B^*$  must be devised. We have been using a real-space charge integration scheme for calculating the effective charges in some insulators with considerable success.<sup>19-21,24,31,34</sup> In this scheme, the charge density along the  $A$ - $B$  bond and the charge contour in a plane containing the  $A$ - $B$  bond are plotted. From the contour map, the boundary between  $A$  and  $B$  is identified. This boundary then defines the effective radii  $r_A$  and  $r_B$  for atoms  $A$  and  $B$ . The sum of  $r_A$  and  $r_B$  equals the bond length  $AB$ . From the self-consistent calculation, the atom-centered charge-density functions  $\rho_A(\mathbf{r})$  and  $\rho_B(\mathbf{r})$  are obtained.<sup>10</sup> The atomic charges  $Q_A$  and  $Q_B$  within the two spheres of radii  $r_A$  and  $r_B$  are obtained by integrating the functions  $\rho_A(\mathbf{r})$  and  $\rho_B(\mathbf{r})$  in the spherical approximation with  $r_A$  and  $r_B$  as integration limits. The difference between the total valence charge in the unit cell and  $Q_A + Q_B$  constitutes the "interstitial charge," which is divided between  $A$  and  $B$  in proportion to the volumes of the spheres. When the apportioned interstitial charges are added to  $Q_A$  and  $Q_B$ , we have the effective charge  $Q_A^*$  and  $Q_B^*$ .

This direct-space integration scheme for effective charges works best for ionic systems where there are very little interstitial charges and the atomic boundary is easy to define. It may not be as accurate in partially covalent compounds such as  $W$  crystals because of the ambiguity in locating a precise atomic boundary and a relatively large amount of interstitial charges. As pointed out before,<sup>19-21</sup> the plot of the charge contour map is crucial in locating the correct interatomic boundary, which is not always at the minimum of the line charge along the bond  $AB$ .

In Figs. 21 and 22, we display the bond charges along the  $AB$  bond and the contour maps in the  $x$ - $z$  plane for the ten  $W$  crystals. The arrows along the bond charge indicate the atomic boundaries in the crystals. In Table IV, we list the effective radii,  $r_A$  and  $r_B$ , the spherical charge  $Q_A$  and  $Q_B$ , the interstitial charge  $Q_{\text{interstitial}}$  and the effective charges  $Q_A^*$ ,  $Q_B^*$  for each  $W$  crystal. Also listed are the  $Q_A^*$ ,  $Q_B^*$ , and FIC calculated by using the Mulliken scheme. As can be seen, the Mulliken result is quite different from the more accurate integration scheme. It tends to underestimate the ionic character of bonding in  $W$  crystals. For example, the Mulliken scheme predicts SiC to be almost totally covalent while the charge distribution in Fig. 21 shows the C atom to have a much larger region of valence charge distribution than Si. Most of the  $W$  crystals show partially ionic, partially covalent character as judged from their FIC values, except for BeO which is highly ionic with a FIC value of 0.95. There is some evidence that the size of the direct band gap correlates with the calculated FIC.

Recently, other methods of calculating effective charges based on the change in polarization induced by small atomic displacement has been suggested. Test calculations in a binary semiconductor such as GaAs (Ref. 88) gives excellent agreement with experiment. That approach is much more elaborate and is quite different from the present direct space integration method. Although the approach we use still has some minor ambiguity in

covalently bonded solids as discussed above, it nevertheless provides a step-by-step recipe for calculating effective charges in any compounds and is physically much more transparent. Our test calculation on GaAs (ZB structure) (Ref. 13) gives  $Q^*$  for Ga to be 1.93 if the "ionic" radii of Ga and As are chosen to be 1.0771 and 1.3709 Å, respectively. However, this effective charge value is very sensi-

tive to the choice of ionic radius which is less clearly defined in a covalent crystal.

## V. OPTICAL PROPERTIES

The calculated imaginary parts of the dielectric function for the ten  $W$  crystals for photon energy up to 40 eV

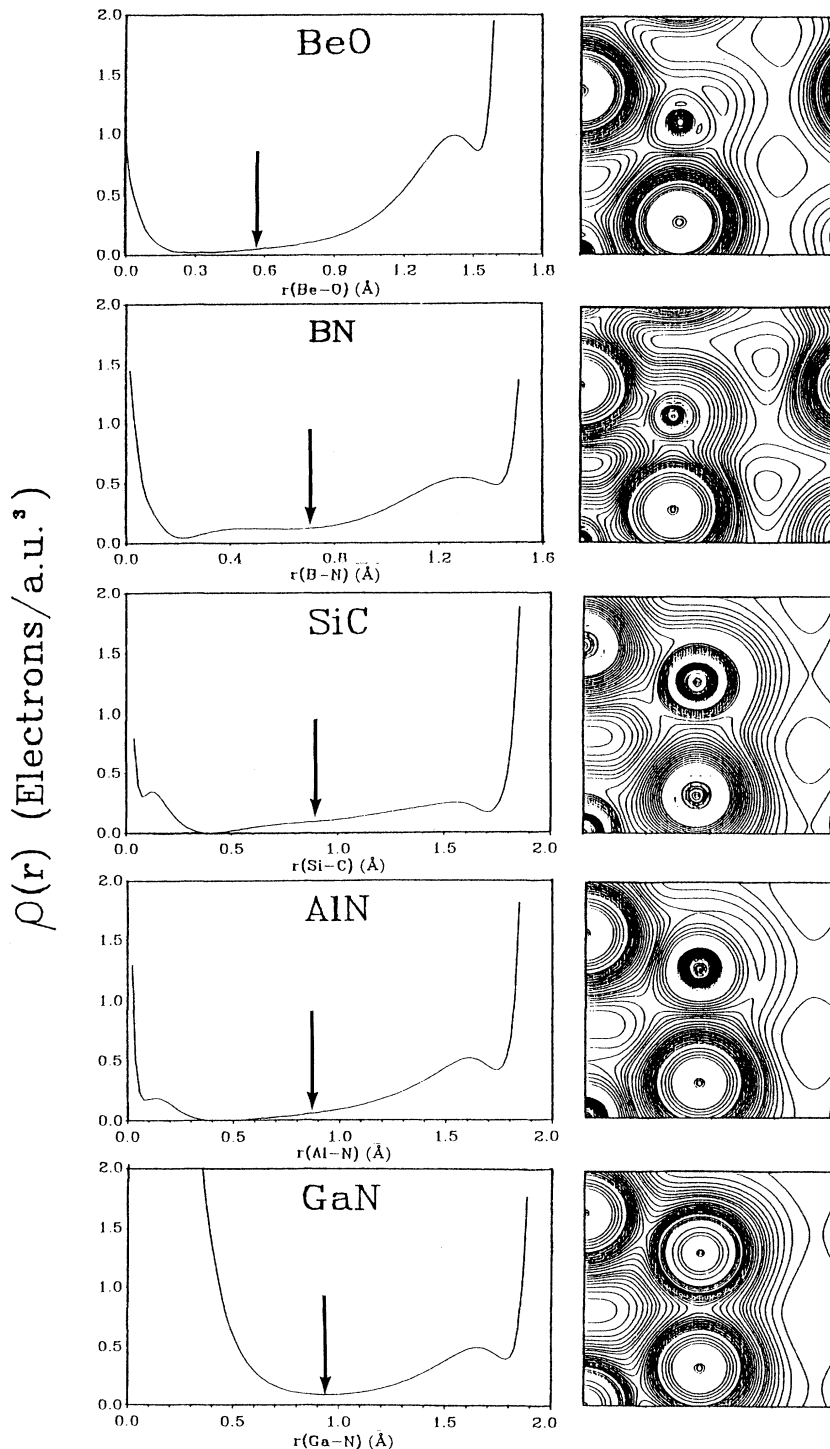


FIG. 21. Charge density along the  $A-B$  bond (left panel) and in the  $x-z$  plane (right panel) for BeO, BN, SiC, AlN, GaN. Units for contour lines: from 0.01 to 0.05 by 0.005; from 0.05 to 0.20 by 0.01; and from 0.20 to 0.40 by 0.05. All in units of electrons/(a.u.)<sup>3</sup>.

are shown in Figs. 23 and 24. The dielectric functions are resolved into two components, the in-plane component  $\epsilon_{xy}(\omega)$  is the average over the  $x$  and the  $y$  directions and the  $z$  component which is perpendicular to  $\epsilon_{xy}(\omega)$ . Since the full calculated spectra are shown, we will not make a detailed analysis or comparison of the spectra. The optical properties of BN and AlN have been discussed in detail elsewhere.<sup>20,43</sup> We will summarize the

optical results of the remaining crystals as follows: (1) The electronic dielectric functions for the ten  $W$  crystals are distinctively different and all have sharp prominent structures depending on the details of the band structures. This indicates that the crystal structure itself, in this case the  $W$  crystal, cannot dictate its optical properties. (2) There is substantial anisotropy in the dielectric functions between the in-plane and the perpendicular

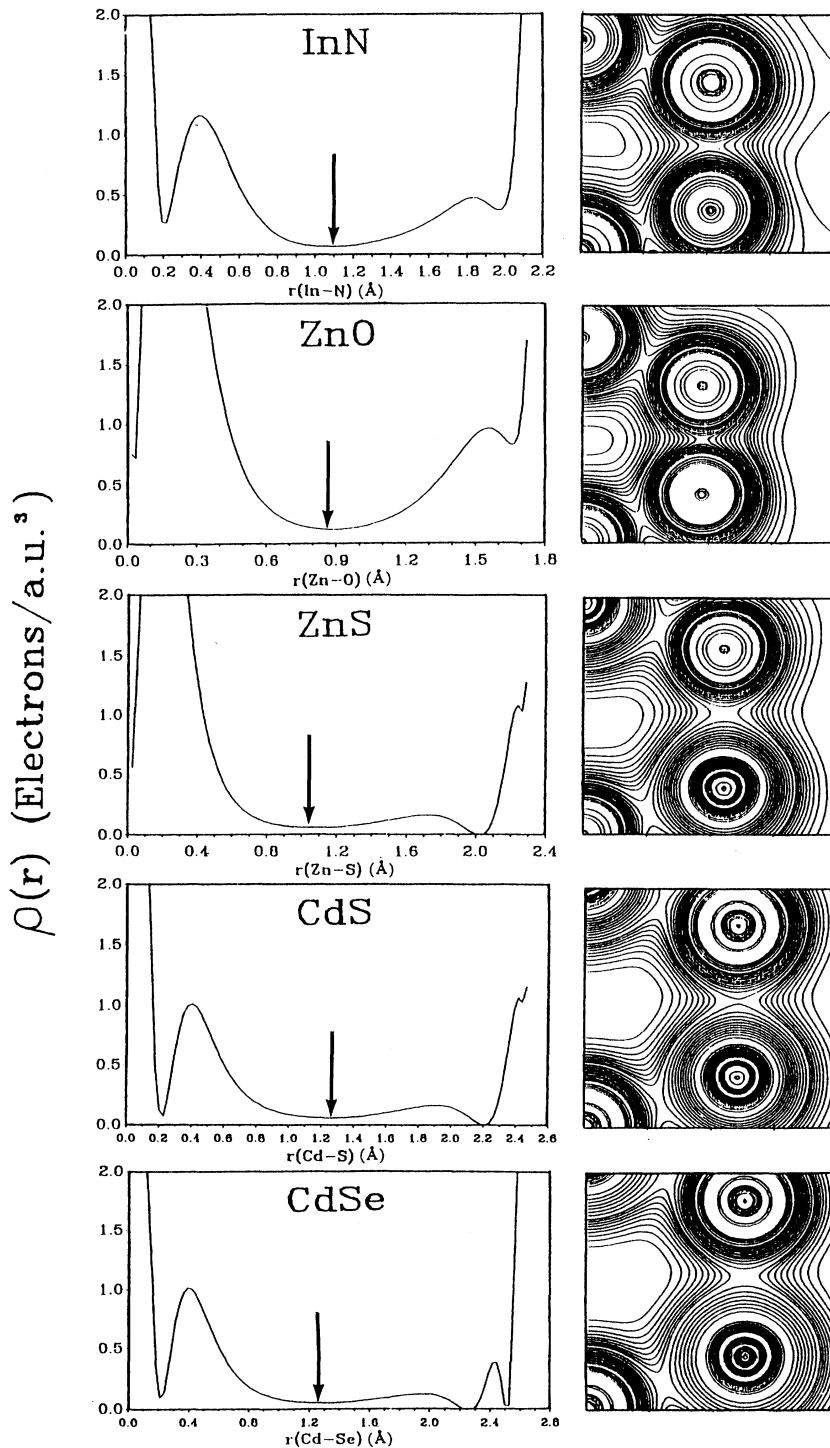


FIG. 22. Charge density along the  $A-B$  bond (left panel) and in the  $x-z$  plane (right panel) for InN, ZnO, ZnS, CdS, CdSe. Contour lines are the same as Fig. 21.

TABLE IV. Calculated effective charges (electrons), ionic radii, and  $FIC = |Q_A^* - Q_B^*| / (Q_A^* + Q_B^*)$  for some wurtzite crystals.

Crystal	$Q_A$ ( $r_A$ in Å)		$Q_B$ ( $r_B$ in Å)		Direct-space integration				Mulliken scheme		
	$Q_A$	$(r_A)$	$Q_B$	$(r_B)$	$Q_{\text{interstitial}}$	$Q_A^*$	$Q_B^*$	FIC	$Q_A^*$	$Q_B^*$	FIC
BeO	0.17	(0.5349)	7.50	(1.1207)	0.33	0.20	7.80	(0.95)	1.76	6.24	(0.56)
BN	1.00	(0.6614)	5.27	(0.9143)	1.73	1.47	6.53	(0.63)	2.99	5.01	(0.25)
SiC	1.53	(0.8834)	4.35	(1.0096)	2.12	2.38	5.62	(0.41)	3.96	4.04	(0.01)
AlN	0.66	(0.8505)	6.00	(1.0523)	1.34	1.12	6.88	(0.72)	2.86	5.14	(0.29)
GaN	1.90	(0.9340)	5.94	(1.0119)	0.16	1.98	6.02	(0.51)	2.80	5.20	(0.43)
InN	1.36	(1.0673)	5.73	(1.0673)	0.91	1.83	6.17	(0.54)	2.70	5.30	(0.45)
ZnO	0.91	(0.8855)	6.49	(0.9108)	0.60	1.20	6.80	(0.70)	1.88	6.12	(0.53)
ZnS	1.70	(1.0672)	6.16	(1.2705)	0.14	1.77	6.23	(0.56)	1.06	6.94	(0.74)
CdS	1.80	(1.2462)	6.10	(1.3988)	0.10	1.85	6.15	(0.54)	1.46	6.54	(0.64)
CdSe	2.30	(1.2770)	5.60	(1.3536)	0.10	2.35	5.65	(0.41)	1.58	6.42	(0.61)

components. This is most evident in SiC. The degree of anisotropy depends on the electronic structure of each crystal. (3) There are substantial absorptions above 20 eV in several crystals, especially in GaN and ZnO. The presence of the semicorelike  $d$  states in different regions of VB precludes a simple interpretation of these structures. (4) There is a reasonable resemblance in the absorption spectra of the nitride series (AlN, GaN, and InN) below 20 eV. This is quite obvious from the similarity of the upper VB and lower CB structures in these three crystals as shown in Figs. 4–6, with the exception of the size of the band gaps. (5) There is also a reasonable resemblance in the spectra for the two sulfides, ZnS and CdS. This is again related to the similarities in the band structures. In ZnS, the Zn  $3d$  level is at  $-6$  eV while in CdS, the Cd  $4d$

level is at  $-10.4$  eV. This indicates that the transitions from the relatively more localized  $d$  states are not important in these two crystals.

The real parts of the dielectric functions  $\epsilon_1(\omega)$  (averaged over the three Cartesian directions) are obtained from the imaginary parts by the Kramers-Kronig conversion and the results for the ten  $W$  crystals are shown in Fig. 25. The most important quantity is the zero frequency limit  $\epsilon(0)$  which is the electronic part of the static dielectric constant. This quantity may be related to the reflective index measured at a frequency above the lattice vibrational frequencies. Our calculated static dielectric constant averaged over the three directions for the ten  $W$  crystals are listed in Table V. They range from a low value of 2.76 for BeO to a larger value of 9.5 for GaN.

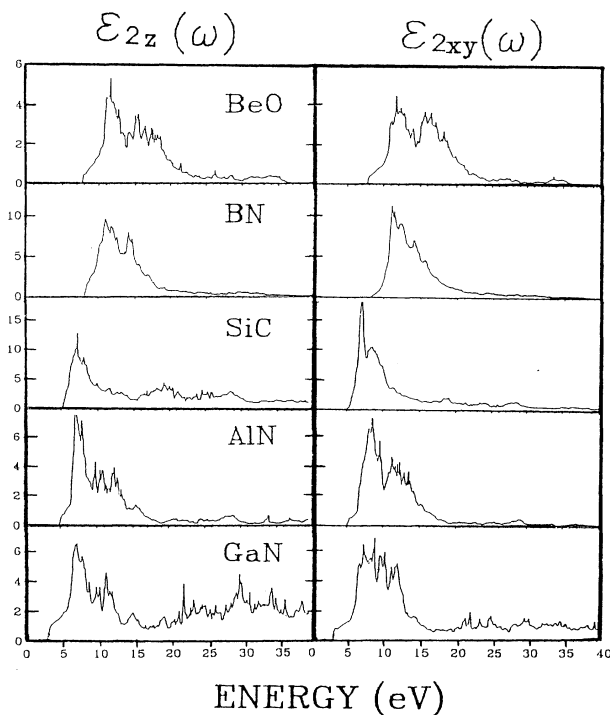


FIG. 23. Imaginary parts of the dielectric functions of BeO, BN, SiC, AlN, GaN: left panel, polarization along the  $z$  axis; right panel, in the  $x$ - $y$  plane.

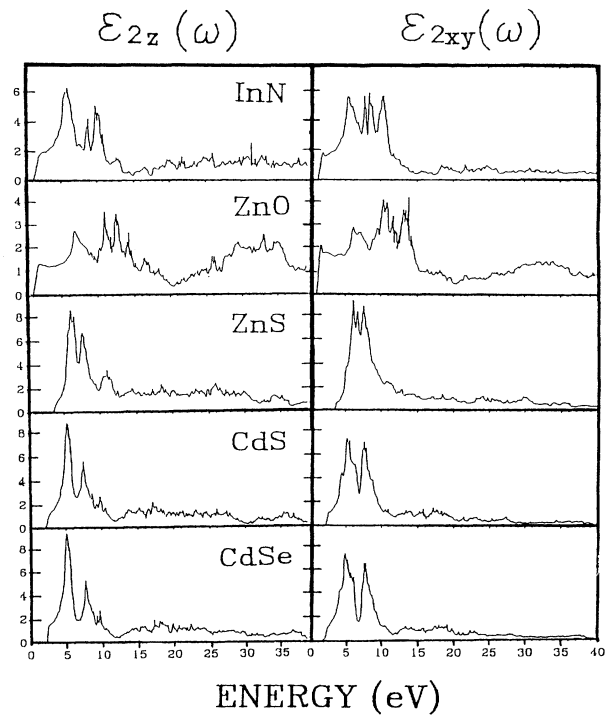


FIG. 24. Imaginary parts of the dielectric functions of InN, ZnO, ZnS, CdS, CdSe: left panel, polarization along the  $z$  axis; right panel, in the  $x$ - $y$  plane.

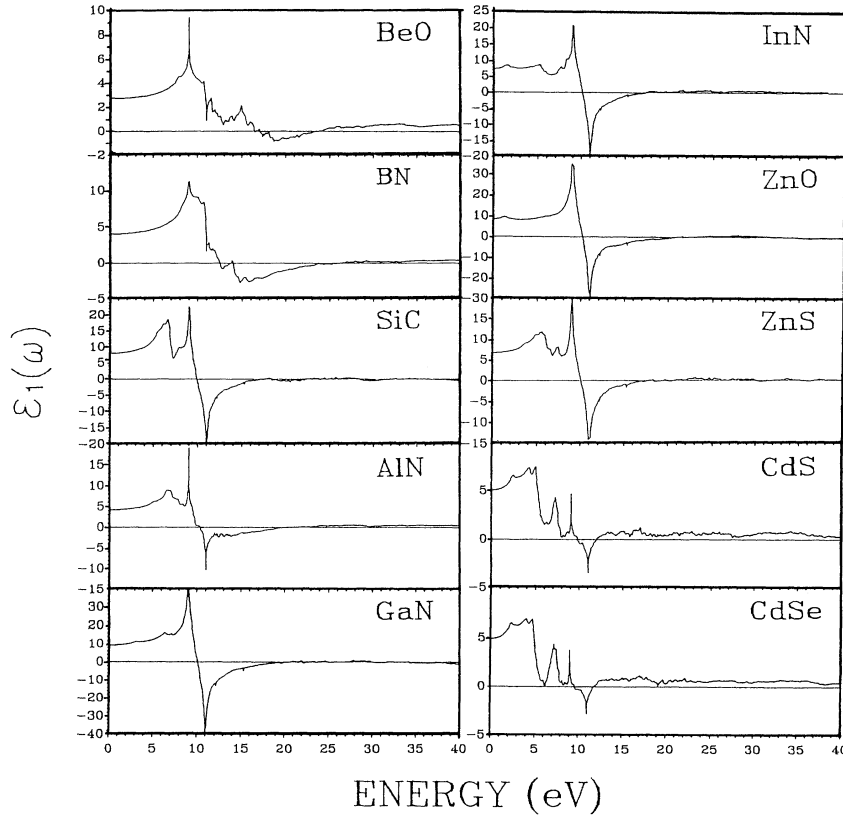


FIG. 25. Real parts of the dielectric functions for ten  $W$  crystals.

The precise determination of the  $\epsilon(0)$  values for these crystals is complicated by the fact that the band gap obtained from the LDA calculation is always underestimated and varies from crystal to crystal. For example, in case of SiC, the perpendicular and parallel components of the electronic portion of the static dielectric constant for 6H SiC were reported to be 6.52 and 6.70, respectively.<sup>89</sup> This is compared with our calculated values of 7.70 and 8.87 for the same two components. Similar linear-optical calculations in cubic semiconductors<sup>13</sup> indicate that underestimation of gaps leads to larger values for  $\epsilon(0)$ . A more elaborate calculation of the dielectric constants using sophisticated correction procedures exists<sup>90–94</sup> and so

far has not been applied to the  $W$  crystals discussed in this paper. In Table V, we have also resolved  $\epsilon(0)$  into in-plane and the perpendicular components in order to estimate the degree of anisotropy for this constant. It can be seen that AlN, GaN, and ZnS have the highest anisotropy  $\Delta\epsilon$ , followed by SiC, InN, and ZnO in that order. In CdS and CdSe,  $\Delta\epsilon$  is small but negative.

Bloom *et al.* measured the reflectivity spectrum of GaN up to 10 eV.<sup>69</sup> The spectrum shows a major peak at 7 eV and several additional structures attributed to critical-point transitions. Our calculated  $\epsilon_2(\omega)$  curve for GaN in Fig. 23, when converted to a reflectivity spectrum, shows good agreement with the data.

TABLE V. Calculated components of electronic dielectric constants and anisotropy factor in wurtzite crystals,  $\epsilon_0 = \frac{1}{3}(\epsilon_x + \epsilon_y + \epsilon_z)$ ,  $\epsilon_{xy} = \frac{1}{2}(\epsilon_x \epsilon_y)$ , and  $\Delta\epsilon = (\epsilon_z - \epsilon_{xy})/\epsilon_0$ , and positions of plasmon peaks.

Crystal	$\epsilon_0$	$\epsilon_{xy}$	$\epsilon_z$	$\Delta\epsilon$	$\omega_p$ (eV)
BeO	2.755	2.747	2.770	0.008	13.5, 23.5, 35.0
BN	4.065	3.982	4.232	0.061	23.4, 26.1, 32.5
SiC	8.090	7.704	8.870	0.144	10.2, 16.3, 22.2, 26.0, 32.0
AlN	4.272	3.876	5.063	0.278	10.2, 20.7, 25.3, 29.5, 33.7, 37.2
GaN	9.530	8.716	11.159	0.256	10.0, 20.0, 26.6, 31.5, 37.2
InN	7.390	7.054	8.061	0.136	6.5, 10.3, 17.1, 26.3
ZnO	8.619	8.331	9.196	0.100	10.3, 17.0, 21.2, 27.5, 32.0, 32.8
ZnS	6.810	6.287	7.866	0.232	10.0, 17.0, 21.2, 27.5, 32.0, 32.8
CdS	5.071	5.082	5.051	-0.006	6.4, 10.0, 12.2, 20.0, 28.4, 39.4
CdSe	4.939	4.947	4.924	-0.005	7.5, 10.3, 12.0, 19.9, 24.5, 29.0, 33.0

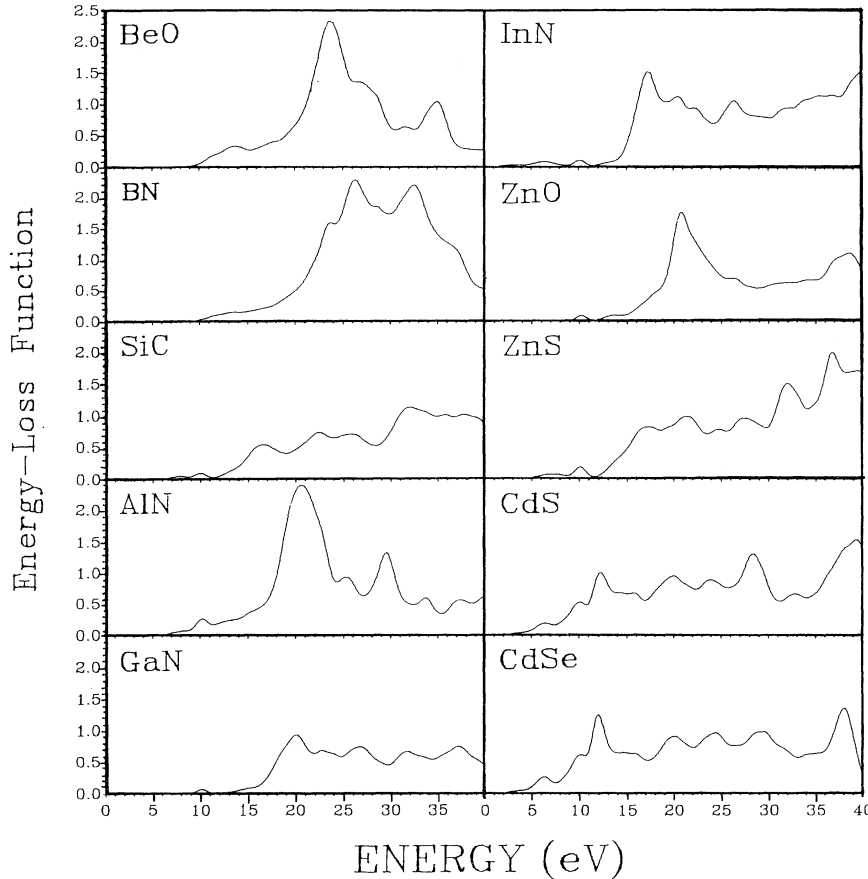


FIG. 26. Electron energy-loss function for the ten wurtzite crystals.

Our calculated  $\epsilon_2(\omega)$  curve for InN is in quite good agreement with the experimental data of Sobolev *et al.*<sup>95</sup> (not shown) which have a deep minimum at 6.5 eV for the perpendicular component of light polarization. For ZnO, the calculated optical spectra in the perpendicular to *c* and parallel to *c* directions are consistent with the measured reflectance data<sup>89</sup> up to photon energy of 16 eV.

The electron energy-loss functions (ELF) for the ten *W* crystals are also calculated from complex dielectric functions and are shown in Fig. 26. Generally speaking, the most prominent peak in the ELF spectrum is identified as the plasmon peak, signaling the energy of collective excitation of the electronic charge density in the crystal. It is possible to have several plasmon peaks in a crystal. From Fig. 26, it can be seen that there are multiple structures in most ELF spectra. Only in BeO, AlN, and Zn can we consider the existence of some prominent peaks. The position of these plasmon peaks are listed in Table V. Additional plasmon peaks above 40 eV cannot be ruled out for some of the *W* crystals.

## VI. TOTAL-ENERGY CALCULATIONS

The OLCAO-LDA method has been successfully used for total-energy calculations to study the ground-state bulk properties in a number of crystals.<sup>11,14,16,20,23</sup> Here, we report a similar calculation for the *W* crystals. As

mentioned earlier, we assume a uniform scaling of lattice constants with the *c/a* ratio fixed, and calculate the total energy as a function of volume. In the total-energy calculation, the accuracy of the fitted charge density must be maintained at a very high level. We have achieved, in general, a fitting accuracy of the order of 0.001 electrons per valence electron. We made no attempt to further optimize the fitting functions or the basis functions. Our past experience and isolated tests indicate that the total-energy result is not very sensitive to a minor variation in the basis function as long as a full basis set is used. It is conceivable that an improved result for total energy may be obtained by further optimizing the fitting functions.

Figure 27 shows the total energy versus  $V/V_0$  curves for the ten *W* crystals. For each crystal, both the actual data points and the curve obtained by fitting the data points to Murnaghan's equation of state<sup>56</sup> are presented. The zero energy per molecule for each curve is set at the calculated minimum and the energy scales for all the curves are the same. It can be seen that the calculated data points are quite smooth with the exception of CdS. The bulk properties from the total-energy calculation are summarized in Table VI, together with some limited experimental data.<sup>95-106</sup> The calculated equilibrium volumes are remarkably close to the measured data. For the bulk modulus *B*, the agreement with the available experimental data is also quite good, particularly in SiC, AlN, GaN, and CdS. However, it should be pointed out

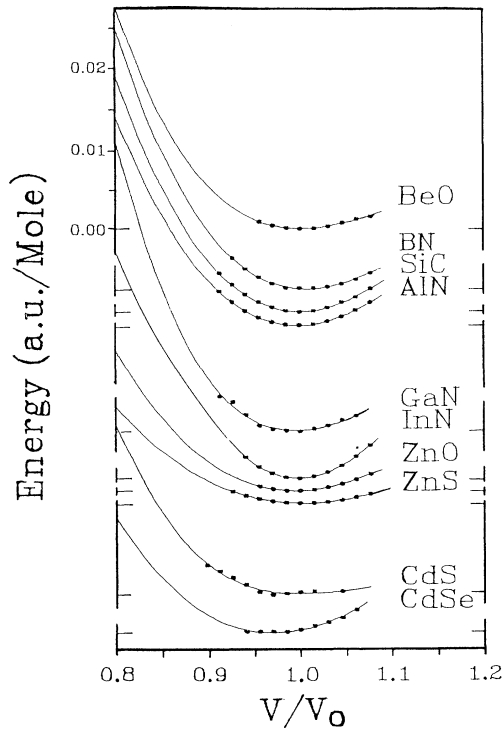


FIG. 27. Total energy as a function of volume for ten wurtzite crystals.

that the  $B$  values derived from such calculations may depend, to a certain extent, on the equation of states used and to a lesser extent on the number of calculated data points. We made no attempt to improve the agreement by a selective choice of data points. Unfortunately, we

are unable to locate the more recent experimental data for  $B$  and  $B'$  for several  $W$  crystals for comparison, and accurate experimental measurements are highly desirable. Table VI also lists the experimental data for pressure coefficient  $B'$  for some crystals. As expected, the pressure coefficient  $B'$  is less accurate than  $B$  both experimentally and theoretically.

For BeO, our calculated bulk modulus of 2.12 Mbar slightly underestimates the measured data.<sup>104,105</sup> On the other hand, the first-principles pseudopotential calculation of Ref. 59 overestimates the measured data. For GaN, our calculated bulk modulus of 2.03 Mbar is very close to the experimental value of 1.95 Mbar.<sup>102</sup> The pseudopotential calculation of MCH gave for  $B$  of GaN 2.4 Mbar.<sup>67</sup> Similar calculations by Muñoz and Kunc in the ZB approximation gave for  $B$  of GaN 1.79 Mbar.<sup>72</sup> For AlN, our calculated bulk property is similar to the earlier one,<sup>14</sup> and is in good agreement with the recent high-pressure experiment by Ueno *et al.*<sup>97</sup> and other data.

A number of researchers have studied the relative stability of the  $W$  crystal against other structures, especially the ZB structure.<sup>57,59,66,72</sup> With the exception of BN, where our total-energy calculation for different phases yields very good results,<sup>20</sup> we have not studied the possible transformation of the  $W$  crystals to other phases under different thermodynamic conditions.

## VII. DISCUSSION

We have presented detailed calculations on the bulk electronic structures, charge-density distributions, linear-optical absorptions, and total-energy results for ten wurtzite crystals. These are all technologically significant materials and a fundamental understanding of their elec-

TABLE VI. Calculated equilibrium volume factors  $V_{\min}/V_0$ , bulk modulus  $B$  (GPa), and pressure coefficient  $B'$  in wurtzite crystals.

Crystal	$V_{\min}/V_0$	$B$ (Mbar)	Experiment	$B'$	Experiment
BeO	1.002	2.12	2.24, <sup>i</sup> 2.29 <sup>j</sup>	1.97	
BN	1.015	3.92		6.38	
SiC	1.000	2.23	2.24 <sup>f</sup>	5.45	
AlN	1.000	2.07	2.08±0.6 <sup>b</sup> 2.02 <sup>c</sup> 2.06 <sup>d</sup>	5.60	6.3±0.9 <sup>b</sup> 6 <sup>c</sup>
GaN	1.000	2.03	1.95 <sup>g</sup> 2.45 <sup>e</sup>	3.98	
InN	1.000	2.12		3.40	
ZnO	1.000	1.25	1.43 <sup>k</sup> 0.85, <sup>a</sup> 0.48 <sup>a</sup>	4.68	4.0, <sup>a</sup> 6.2 <sup>a</sup>
ZnS	1.000	0.50	0.78 <sup>k</sup> 0.762 <sup>h</sup>	4.02	4.37±0.07 <sup>h</sup>
CdS	0.970	0.60	0.61 <sup>k</sup>	12.4	
CdSe	0.975	0.58	0.53 <sup>k</sup>	3.17	

<sup>a</sup>Reference 96.

<sup>b</sup>Reference 97.

<sup>c</sup>Reference 98.

<sup>d</sup>Reference 99.

<sup>e</sup>Reference 100.

<sup>f</sup>Reference 101.

<sup>g</sup>Reference 102.

<sup>h</sup>Reference 103.

<sup>i</sup>Reference 104.

<sup>j</sup>Reference 105.

<sup>k</sup>Reference 106.

tronic properties is important. We believe this is the most comprehensive study to date for wurtzite crystals and the results obtained are in good agreement with experimental data. The band structures obtained are more accurate than earlier calculations using a semi-*ab-initio* OLCAO approach.<sup>2</sup> With the exception of AlN and GaN, experimental results on other wurtzite crystals appear to be very limited. Our first-principles calculation will certainly be very useful for the interpretation of future experiments. We intend to use the present results on ideal perfect crystals as a starting point for future studies on more realistic systems involving defects, impurities, interfaces, and superlattice structures of these crystals. Also of interest is the change of electronic structures and optical properties of *W* crystals under pressure.

Recently, we studied the nonlinear optical properties of 18 cubic semiconductors.<sup>107-109</sup> The dispersion relations for the second-harmonic and third-harmonic generations

were calculated with zero frequency limits in good agreement with experiment. Since most of the *W* crystals studied here and their more complicated alloys and other structural configurations may have great potential in electro-optical technology, it is natural to extend nonlinear optical calculations to these *W* crystals. As a matter of fact, the nonlinear optical properties of some *W* crystals were studied almost 20 years ago, albeit by rather crude empirical approaches.<sup>110-113</sup> To our knowledge, no reasonably detailed nonlinear optical calculations for *W* crystals have existed in the last two decades. Clearly, the direct-space OLCAO method is fully capable of meeting such a challenge.

#### ACKNOWLEDGMENT

This work was supported by the U.S. Department of Energy under Grant No. DE-FG02-84ER45170.

- <sup>1</sup>M. L. Cohen and J. R. Chelikowsky, *Electronic Structure and Optical Properties of Semiconductors* (Springer-Verlag, New York, 1988).
- <sup>2</sup>M.-Z. Huang and W. H. Ching, *J. Phys. Chem. Solids* **46**, 977 (1985).
- <sup>3</sup>W. H. Ching, M.-Z. Huang, and D. L. Huber, *Phys. Rev. B* **29**, 2337 (1984).
- <sup>4</sup>W. Y. Ching and M.-Z. Huang, *Superlatt. Microstruct.* **1**, 141 (1985).
- <sup>5</sup>M.-Z. Huang and W. Y. Ching, *Superlatt. Microstruct.* **1**, 137 (1985).
- <sup>6</sup>W. Y. Ching and M.-Z. Huang, *Solid State Commun.* **57**, 305 (1986).
- <sup>7</sup>Y.-P. Li and W. Y. Ching, *Phys. Rev. B* **31**, 2172 (1985).
- <sup>8</sup>D. J. Moss, J. E. Sipe, and H. M. van Driel, *Phys. Rev. B* **36**, 9708 (1987).
- <sup>9</sup>D. J. Moss, E. Ghahramani, J. E. Sipe, and H. M. van Driel, *Phys. Rev. B* **41**, 1542 (1990).
- <sup>10</sup>W. Y. Ching, *J. Am. Ceram. Soc.* **71**, 3135 (1990), and references cited therein.
- <sup>11</sup>F. Zandiehnam and W. Y. Ching, *Phys. Rev. B* **41**, 493 (1990).
- <sup>12</sup>W. Y. Ching, Y.-N. Xu, and K. W. Wong, *Phys. Rev. B* **40**, 7684 (1989).
- <sup>13</sup>M.-Z. Huang and W. Y. Ching, *Phys. Rev. B* **47**, 9449 (1993).
- <sup>14</sup>W. Y. Ching and B. N. Harmon, *Phys. Rev. B* **34**, 5305 (1986).
- <sup>15</sup>Y.-N. Xu and W. Y. Ching, *Physica* **150B**, 32 (1988); F. Zandiehnam, R. A. Murray, and W. Y. Ching, *ibid.* **150B**, 19 (1988).
- <sup>16</sup>Y.-N. Xu and W. Y. Ching, in *SiO<sub>2</sub> and its Interfaces*, edited by S. T. Pantelides and G. Lacosky, MRS Symposia Proceedings No. 105 (Materials Research Society, Pittsburgh, 1988).
- <sup>17</sup>J. C. Parker, D. J. Lam, Y.-N. Xu, and W. Y. Ching, *Phys. Rev. B* **42**, 5289 (1990).
- <sup>18</sup>J. C. Parker, U. W. Gelsler, D. J. Lam, Y.-M. Xu, and W. Y. Ching, *J. Am. Ceram. Soc.* **71**, 3206 (1990).
- <sup>19</sup>W. Y. Ching and Y.-N. Xu, *Phys. Rev. Lett.* **65**, 895 (1990).
- <sup>20</sup>Y.-N. Xu and W. Y. Ching, *Phys. Rev. B* **44**, 7787 (1991).
- <sup>21</sup>Y.-N. Xu and W. Y. Ching, *Phys. Rev. B* **43**, 4461 (1991).
- <sup>22</sup>Y.-N. Xu and W. Y. Ching, *Phys. Rev. B* **44**, 11 048 (1991).
- <sup>23</sup>D. Li, Y.-N. Xu, and W. Y. Ching, *Phys. Rev. B* **45**, 5895 (1992).
- <sup>24</sup>F. Gan, M.-Z. Huang, Y.-N. Xu, W. Y. Ching, and J. G. Harrison, *Phys. Rev. B* **45**, 8248 (1992).
- <sup>25</sup>W. Y. Ching, Y.-N. Xu, G. L. Zhao, K. W. Wong, and F. Zandiehnam, *Phys. Rev. Lett.* **59**, 1333 (1987).
- <sup>26</sup>G.-L. Zhao, Y.-N. Xu, W. Y. Ching, and K. W. Wong, *Phys. Rev. B* **36**, 7203 (1987).
- <sup>27</sup>W. Y. Ching, G.-L. Zhao, Y.-N. Xu, and K. W. Wong, *Mod. Phys. Lett. B* **3**, 263 (1989).
- <sup>28</sup>G.-L. Zhao, W. Y. Ching, and K. W. Wong, *J. Opt. Soc. Am. B* **6**, 505 (1989).
- <sup>29</sup>Y.-N. Xu, W. Y. Ching, and K. W. Wong, *Phys. Rev. B* **37**, 9773 (1988).
- <sup>30</sup>W. Y. Ching, G.-L. Zhao, Y.-N. Xu, and K. W. Wong, *Phys. Rev. B* **43**, 6159 (1991).
- <sup>31</sup>Y.-N. Xu, W. Y. Ching, and R. H. French, *Ferroelectrics* **111**, 23 (1990).
- <sup>32</sup>Y.-N. Xu and W. Y. Ching, *Phys. Rev. B* **41**, 5471 (1990).
- <sup>33</sup>W. Y. Ching and Y.-N. Xu, *Phys. Rev. B* **44**, 5332 (1991).
- <sup>34</sup>H. Jiang, Y.-N. Xu, and W. Y. Ching, *Ferroelectrics* **136**, 137 (1992).
- <sup>35</sup>W. Y. Ching, Y.-N. Xu, B. N. Harmon, J. Ye, and C. T. Leung, *Phys. Rev. B* **42**, 4460 (1990).
- <sup>36</sup>X.-F. Zhong, Y.-N. Xu, and W. Y. Ching, *Phys. Rev. B* **41**, 10 545 (1990).
- <sup>37</sup>W. Y. Ching, M.-Z. Huang, Y.-N. Xu, W. G. Harter, and F. T. Chan, *Phys. Rev. Lett.* **67**, 2045 (1991).
- <sup>38</sup>Y.-N. Xu, M.-Z. Huang, and W. Y. Ching, *Phys. Rev. B* **44**, 13 171 (1991).
- <sup>39</sup>M.-Z. Huang, Y.-N. Xu, and W. Y. Ching, *J. Chem. Phys.* **96**, 1648 (1992); *Phys. Rev. B* **47**, 3221 (1993).
- <sup>40</sup>Y.-N. Xu, M.-Z. Huang, and W. Y. Ching, *Phys. Rev. B* **46**, 6572 (1992).
- <sup>41</sup>W. Y. Ching, M.-Z. Huang, and Y.-N. Xu, *Phys. Rev. B* **46**, 9910 (1992).
- <sup>42</sup>M.-Z. Huang, W. Y. Ching, and T. Lenosky, *Phys. Rev. B* **47**, 1593 (1993).
- <sup>43</sup>S. Loughin, R. H. French, W. Y. Ching, Y.-N. Xu, and G. A. Slack (unpublished).
- <sup>44</sup>See, for example, *Synthesis and Properties of Boron Nitride*, edited by J. J. Pouch and S. A. Alteroviz (Trans Tech., Aedermannsdorf, Switzerland, 1990).
- <sup>45</sup>See, for example, *Amorphous and Crystalline Silicon Carbide and Related Materials*, edited by G. L. Harris and C. Y.-W.



- Yang, *Proceedings in Physics* Vol. 34 (Springer, Berlin, 1989).
- <sup>46</sup>S. Strite and H. Morkoc, *J. Vac. Sci. Technol. B* **10**, 1237 (1992).
- <sup>47</sup>N. Kuramoto, H. Taniguchi, I. Aso, *Ceram. Bull.* **68**, 883 (1989).
- <sup>48</sup>C. R. Aita, C. J. G. Kubiak, and F. Y. H. Shih, *J. Appl. Phys.* **66**, 4360 (1980).
- <sup>49</sup>T. Shiosaki, in *Proceedings of the IEEE Ultrasonic Symposium*, edited by J. deKlerk and B. R. McAvoy (IEEE, New York, 1978), p. 100.
- <sup>50</sup>M. Matsuoka and K. Ono, *J. Vac. Sci. Technol. A* **7**, 2975 (1989).
- <sup>51</sup>M. A. Haase, H. Cheng, D. K. Misemer, T. A. Strand, and J. M. DePuydt, *Appl. Phys. Lett.* **59**, 3228 (1991).
- <sup>52</sup>*Handbook of Laser Science and Technology*, edited by M. J. Weber (CRC, Cleveland, 1986), Vol. III.
- <sup>53</sup>W. Kohn and L. J. Sham, *Phys. Rev.* **140**, A1133 (1965); L. J. Sham and W. Kohn, *ibid.* **145**, 561 (1965).
- <sup>54</sup>E. Wigner, *Phys. Rev.* **46**, 1002 (1934).
- <sup>55</sup>G. Lehmann and M. Taut, *Phys. Status Solidi* **54**, 469 (1972); O. Jesen and O. K. Anderson, *Solid State Commun.* **9**, 1763 (1971).
- <sup>56</sup>F. D. Murnaghan, *Proc. Natl. Acad. Sci. U.S.A.* **30**, 244 (1944).
- <sup>57</sup>C.-Y. Yeh, Z. W. Lu, S. Froyen, and A. Zunger, *Phys. Rev. B* **46**, 10086 (1992).
- <sup>58</sup>K. J. Chang, S. Froyen, and M. L. Cohen, *J. Phys. C* **16**, 3475 (1983).
- <sup>59</sup>K. J. Chang and M. L. Cohen, *Solid State Commun.* **50**, 487 (1984).
- <sup>60</sup>A. Contineza, R. M. Wentzcovitch, and A. J. Freeman, *Phys. Rev. B* **41**, 3540 (1990).
- <sup>61</sup>M. Posternak, A. Baldereschi, A. Catellani, and R. Resta, *Phys. Rev. Lett.* **64**, 1777 (1990).
- <sup>62</sup>K. T. Park, K. Terakura, and N. Hamada, *J. Phys. C* **20**, 1241 (1987).
- <sup>63</sup>P. K. Lam, R. M. Wentzcovitch, and M. L. Cohen, *Mater. Sci. Forum* **54-55**, 165 (1990).
- <sup>64</sup>W. R. L. Lambrecht and B. Segall, in *Wide Band-Gap Semiconductors*, edited by T. D. Moustakis, J. I. Pankove, and Y. Hamakawa, MRS Symposia Proceedings No. 242 (Materials Research Society, Pittsburgh, 1992).
- <sup>65</sup>I. Gorczyca, N. E. Christensen, P. Perlin, I. Grezegory, J. Jun, and M. Bockowski, *Solid State Commun.* **79**, 1033 (1991).
- <sup>66</sup>P. E. Van Camp, V. E. Doren, and J. T. Devreese, *Phys. Rev. B* **44**, 9056 (1991).
- <sup>67</sup>B. J. Min, C. T. Chan, and K. M. Ho, *Phys. Rev. B* **45**, 1159 (1992).
- <sup>68</sup>S. N. Grinyaev, V. Ya. Malakhov, and V. A. Chaldyshev, *Izv. Vyssh. Uchebn. Zaved. Fiz.* **28**, 3 (1985) [*Sov. Phys. J.* **28**, 251 (1985)].
- <sup>69</sup>S. Bloom, G. Harbeke, E. Meier, and I. B. Ortenburger, *Phys. Status Solidi B* **66**, 161 (1974).
- <sup>70</sup>D. Jones and A. H. Lettington, *Solid State Commun.* **11**, 701 (1972).
- <sup>71</sup>P. Perlin, I. Gorczyca, N. E. Christensen, I. Grezegory, H. Teisseyre, and T. Suski, *Phys. Rev. B* **45**, 11 307 (1992).
- <sup>72</sup>A. Muñoz and K. Kunc, *Phys. Rev. B* **44**, 10 372 (1991).
- <sup>73</sup>C. P. Foley and T. L. Tansley, *Phys. Rev. B* **33**, 1430 (1986).
- <sup>74</sup>D. W. Jenkins and J. D. Dow, *Phys. Rev. B* **39**, 3317 (1989).
- <sup>75</sup>S. Bloom and I. Ortenberger, *Phys. Status Solidi* **58**, 561 (1973).
- <sup>76</sup>J. R. Chelikowsky, *Solid State Commun.* **22**, 351 (1977).
- <sup>77</sup>K. C. Mishra, P. C. Schmidt, K. H. Johnson, B. G. Deboer, J. K. Berkowitz, and E. A. Dale, *Phys. Rev. B* **42**, 1423 (1990).
- <sup>78</sup>T. K. Bergstresser and M. L. Cohen, *Phys. Lett.* **23**, 8 (1966).
- <sup>79</sup>T. K. Bergstresser and M. L. Cohen, *Phys. Rev.* **164**, 1069 (1967).
- <sup>80</sup>M. L. Cohen, in *II-VI Semiconducting Compounds*, edited by D. G. Thomas (Benjamin, New York, 1967), p. 462.
- <sup>81</sup>P. B. Berry and R. F. Rutz, *Appl. Phys. Lett.* **33**, 319 (1978).
- <sup>82</sup>B. Monemar, *Phys. Rev. B* **10**, 676 (1974).
- <sup>83</sup>R. B. Zetterstram, *J. Mater. Sci.* **5**, 1102 (1970).
- <sup>84</sup>L. Ley, R. A. Pollak, F. R. McFeely, S. P. Kowalczyk, and D. A. Shireley, *Phys. Rev. B* **9**, 600 (1974).
- <sup>85</sup>T. L. Tansley and C. P. Foley, *Electron. Lett.* **20**, 1066 (1984).
- <sup>86</sup>J. C. Phillips, *Bonds and Bands in Semiconductors* (Academic, New York, 1973), p. 31.
- <sup>87</sup>R. S. Mulliken, *J. Am. Chem. Soc.* **77**, 887 (1954).
- <sup>88</sup>R. D. King-Smith and D. Vanderbilt, *Phys. Rev. B* **47**, 1651 (1993).
- <sup>89</sup>L. Patrick and W. J. Choyke, *Phys. Rev. B* **2**, 2255 (1970).
- <sup>90</sup>M. S. Hybertsen and S. G. Louie, *Phys. Rev. B* **34**, 5390 (1986).
- <sup>91</sup>C. S. Wang and W. E. Pickett, *Phys. Rev. Lett.* **51**, 597 (1983); *Phys. Rev. B* **30**, 4719 (1984).
- <sup>92</sup>R. W. Godby, M. Schluter, and L. J. Sham, *Phys. Rev. Lett.* **56**, 2415 (1986); *Phys. Rev. B* **36**, 6497 (1987); **37**, 10 159 (1988).
- <sup>93</sup>F. Bechstedt and R. Del Sole, *Phys. Rev. B* **38**, 7710 (1988).
- <sup>94</sup>Z. H. Levine and D. C. Allan, *Phys. Rev. Lett.* **63**, 1719 (1989); *Phys. Rev. B* **44**, 12 781 (1991).
- <sup>95</sup>V. Sobolev, S. G. Kroitu, A. F. Andreeva, and V. Ya. Malakhov, *Fiz. Tekh. Poluprovodn.* **13**, 823 (1979) [*Sov. Phys. Semicond.* **13**, 485 (1979)].
- <sup>96</sup>Y. Zhou, A. J. Campbell, and D. L. Heinz, *J. Phys. Chem. Solids* **52**, 821 (1991).
- <sup>97</sup>M. Ueno, A. Onodera, O. Shimomura, and K. Takemura, *Phys. Rev. B* **45**, 10 123 (1992).
- <sup>98</sup>K. Tsubouchi, K. Sugai, and N. Mikoshiba, in *1981 Ultrasonic Symposium Proceedings*, edited by B. R. McAvoy (IEEE, New York, 1981), p. 375.
- <sup>99</sup>P. Boch, J. C. Glandus, J. Jarrige, J. P. Lecompte, and J. Mexmain, *Cerm. Ind. (Chicago)* **8**, 34 (1982).
- <sup>100</sup>P. Berlin, C. Jauberthie-Carillon, J. P. Itie, A. San Migule, I. Grezegory, and A. Polian, *High Pressure Res.* **7**, 76 (1991).
- <sup>101</sup>*Numerical Data and Functional Relationships in Science and Technology*, edited by O. Madelung, Landolt-Börnstein, New Series, Group III, Vol. 17, Pt. a (Springer, Berlin, 1982).
- <sup>102</sup>D. Gerlich, S. L. Dole, and G. A. Slack, *J. Phys. Chem. Solids* **47**, 437 (1986).
- <sup>103</sup>E. Chang and G. R. Barsch, *J. Phys. Chem. Solids* **34**, 1543 (1973).
- <sup>104</sup>G. G. Bente, *J. Am. Ceram. Soc.* **49**, 125 (1966).
- <sup>105</sup>C. F. Cline, H. L. Durmegan, and G. W. Henderson, *J. Appl. Phys.* **38**, 1944 (1967).
- <sup>106</sup>C. F. Cline and D. R. Stephens, *J. Appl. Phys.* **36**, 2869 (1965).
- <sup>107</sup>M.-Z. Huang and W. Y. Ching, *Phys. Rev. B* **45**, 8738 (1992).
- <sup>108</sup>M.-Z. Huang and W. Y. Ching, *Phys. Rev. B* **47**, 9464 (1993).
- <sup>109</sup>W. Y. Ching and M.-Z. Huang, *Phys. Rev. B* **47**, 9479 (1993).
- <sup>110</sup>C. Flytzanis, *C. R. Acad. Sci. Ser. B* **267**, 555 (1968).
- <sup>111</sup>J. C. Phillips and J. A. Van Vechten, *Phys. Rev.* **183**, 709 (1969).
- <sup>112</sup>B. F. Levine, *Phys. Rev. Lett.* **22**, 787 (1969); **25**, 440 (1970).
- <sup>113</sup>B. F. Levine, *Phys. Rev. B* **7**, 2600 (1973).